Earthquake Hazard and Risk Assessment

and

Water-Induced Landslide Hazard

in Benton County, Oregon

Final Report

Zhenming Wang
Gregory B. Graham
Ian P. Madin

Oregon Department of Geology and Mineral Industries
800 NE Oregon Street, #28
Portland, OR 97202

June 2001

INTRODUCTION

Earthquakes and landslides pose great risks to Oregonians. Over the last 15 years, scientists have learned that Oregon has experienced many damaging earthquakes in the past (Atwater, 1987; Heaton and Hartzell, 1987; Weaver and Shedlock, 1989). Great Cascadia subduction earthquakes have occurred many times in the past, most recently on January 26, 1700 (Clague and others, 2000). In addition, shallow crustal earthquakes like the 1993 Scotts Mills earthquake (M 5.6) (Madin and others, 1993) and the 1993 Klamath Falls earthquakes (M 5.9 and 6.0) (Wiley and others, 1993), which caused more than $30 million and $10 million damage, respectively, threaten communities in Oregon. Many parts of Oregon are also highly susceptible to landslide hazard (Beaulieu, 1976), especially in the western part of the state where conducive geological conditions on steep slopes are coupled with abundant precipitation (Burns, 1998a). In February 1996, a storm event caused $10 million in damage in the Portland metropolitan area alone, approximately 40 percent of which was associated with landslides (Burns, 1998b).

Earthquake Hazard and Risk Assessment

Although earthquakes cannot be prevented or predicted, the earthquake hazards can be assessed on the basis of geologic, geophysical, geotechnical, hydrologic, and topographic information. The probabilistic seismic hazard maps developed by Geomatrix Consultants, Inc. (1995) and the U.S. Geological Survey (Frankel and others, 1997) assess general ground shaking hazard on bedrock sites in Oregon. The Oregon Department of Geology and Mineral Industries (DOGAMI) publication GMS-100 depicts probabilistic ground shaking hazard in Oregon, including Benton County, at 500-, 1,000-, and 5,000-year return periods (Madin and Mabey, 1996). These maps provide a general seismic hazard level for the State of Oregon. The ground motion design level in the State of Oregon 1998 edition of the *Structural Specialty Code* (Oregon Building Codes Division, 1998) is based on these probabilistic seismic hazard assessments. Figure 1 shows the peak ground acceleration on bedrock sites at a 500-year return interval in Benton County (Frankel and others, 1997). In addition, ground shaking from a great Cascadia subduction earthquake would be of long period and long duration (Clague and others, 2000).

It is well documented that earthquake hazards are also affected by local geologic, hydrologic, and topographic conditions. Three phenomena generally will be induced by ground shaking during a strong earthquake: (1) amplification of ground shaking by a “soft” soil column; (2) liquefaction of water-saturated sand, silt, or gravel, creating areas of “quicksand;” and (3) landslides, including rock falls and rock slides, triggered by shaking, even on relatively gentle slopes. The following are specific examples of the impact of local conditions on earthquake hazard: (1) Amplified ground motion by near-surface soft soils resulted in great damage in Mexico City during the 1985 Mexico earthquake (Seed and others, 1988). (2) Severe damage in the Marina district of San Francisco was also caused by amplified ground motion and by liquefaction during the 1989 Loma Prieta earthquake (Holzer, 1994). (3) A large rock slide on the east side of U.S. Highway 97 about 2.9 km south of Modoc Point, which hit a southbound vehicle and killed the driver, was induced by the September 1993 Klamath Falls earthquake (Keefer and Schuster, 1993).

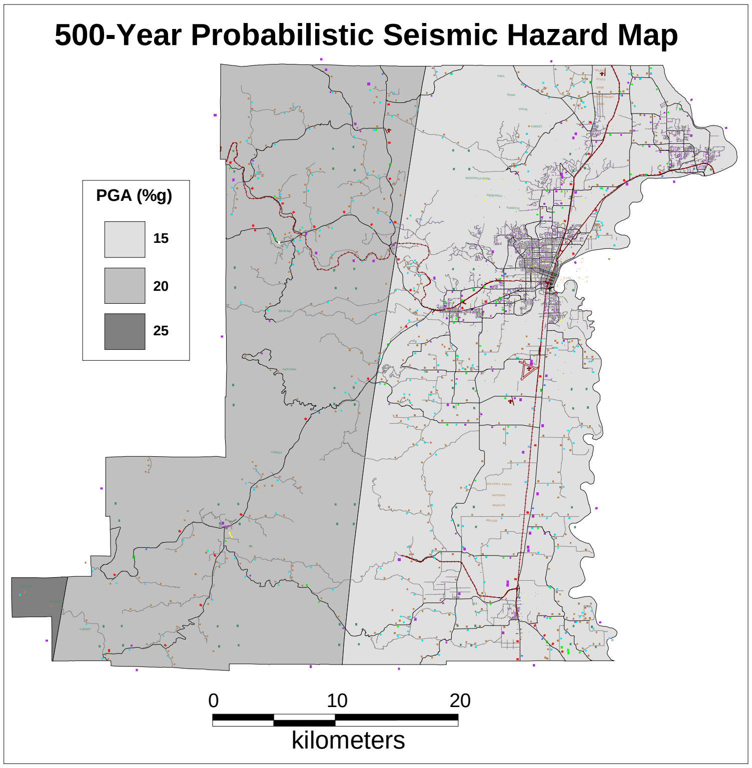

Figure 1. Peak ground acceleration (PGA) expected in Benton County, Oregon, with a frequency of occurrence of once in 500 years (Frankel and others, 1997).

Ground motion amplification, liquefaction potential, and landslide/rockfall potential can be evaluated if the nature and properties of the geologic materials and soils at the sites are known (Bolt, 1993). DOGAMI has made great efforts to evaluate these three effects and has published many hazard maps based on the local geologic, hydrologic, and topographic conditions for many communities in Oregon (Black and others, 2000a and b; Hofmeister and others, 2000a and b; Mabey and others, 1995a, b, c, and d; Madin and Wang, 1999a, b, c, and d; Wang and Leonard, 1996;). These *Relative Earthquake Hazard Maps* depict the ground motion amplification, liquefaction potential, and earthquake-induced landslide/rockfall potential due to local conditions.

A preliminary seismic risk assessment for Benton County indicated that a M 8.5 Cascadia subduction zone earthquake could cause about 400 injuries and deaths and $630 million in building losses (Wang and Clark, 1999). This preliminary study used HAZUS97, a seismic-risk-assessment software package developed by the Federal Emergency Management Agency (FEMA, 1997). The default building inventory and other data contained in HAZUS97 were supplemented with soil information estimated from a state-wide geologic map. The default data did not include unreinforced masonry (URM) buildings. In this study, an improved seismic-risk-assessment software package, HAZUS99, also developed by the Federal Emergency Management Agency (FEMA, 1999), was used to assess seismic risk in Benton County with better seismic hazard and building inventory data.

Water-Induced Landslide Hazard

The term landslide denotes "the movement of a mass of rock, debris, or earth down a slope" (National Research Council, 1996). It includes such phenomena as rock falls, debris flows, earth slides, and others (National Research Council, 1996). Common landslide triggers include intense rainfall, rapid snowmelt, water-level changes, volcanic eruptions, and strong ground shaking during earthquakes (National Research Council, 1996). Landslides triggered by water-related factors are complicated and can be classified in terms of state of activity (e.g., active vs. inactive landslides), distribution of activity (e.g., retrogressive vs. progressive landslides), and style of activity (e.g., complex or single landslides) (National Research Council, 1996). Types of landslides are largely differentiated by material properties, shear plane geometry, and triggering mechanisms. As a result, the analyses used to model or characterize different types of landslides vary and depend on site-specific conditions. Generally, landslide occurrence is determined by local topographic, hydrologic, and geologic conditions.

"An ideal landslide hazard map should provide information concerning the spatial and temporal probabilities of all anticipated landslide types within the mapped area, and also include information about their types, magnitudes, velocities, and sizes" (National Research Council, 1996). Landslide hazard mapping requires (1) a detailed inventory of slope processes, (2) the study of those processes in relation to their environmental setting, (3) the analysis of conditioning and triggering factors, and (4) a representation of the spatial distribution of these factors (National Research Council, 1996). The level of detail in a landslide hazard map is dependent upon scale that can be national (less than 1:1 million), regional (1:50,000 to 1:500,000), medium (1:25,000 to 1:50,000), or large (1:5,000 to 1:15,000). DOGAMI has published many landslide hazard maps at regional and medium scales such as *Environmental Geology of the Coastal Region of Tillamook and Clatsop Counties, Oregon* (Schlicker and others, 1972), *Environmental Geology of Inland Tillamook and Clatsop Counties, Oregon* (Beaulieu, 1973), and landslide susceptibility maps for the western portion of the Salem Hills, Marion County, and the eastern portion of the Eola Hills, Polk County (Harvey and Peterson, 1998 and 2000).

In the present study for Benton County, a GIS-based landslide hazard mapping technique was used to delineate landslide susceptibility triggered by the water-related factors at regional scales (1:50,000 to 1:500,000) on the basis of (1) a landslide inventory and (2) infinite slope modeling. In order to differentiate from earthquake-induced landslides, landslide hazard delineated in this project is called *Water-Induced Landslide Hazard*.

The information from the *water-induced landslide hazard* mapping, and the seismic hazard and risk assessment will help local governments, land use planners, and emergency managers to prioritize areas for hazard mitigation and risk reduction. This preliminary report provides the results from relative seismic hazard mapping, building inventory investigation, seismic risk analysis, and landslide hazard mapping for Benton County.

RELATIVE SEISMIC HAZARD MAPPING

The first step in a relative earthquake hazard evaluation is the development of a geologic model for the study area. The types of relative hazards present in a particular area vary with the spatial distribution of geologic materials and other factors such as topography and hydrologic conditions. For ground motion amplification and liquefaction hazard analysis, the physical characteristics, spatial distribution, and thickness of the unconsolidated sediments overlying bedrock are of primary concern. For analysis of earthquake-induced landslide hazard, slope may well be the most important factor, but bedrock geology (for slopes >25°) and the physical properties of the soils overlying bedrock (for slopes 5°–25°) are both significant in any dynamic slope-stability analysis.

Surface and subsurface geologic, geophysical, geotechnical, and water well data were used to generate a three-dimensional geologic model with the help of the GIS software MapInfo™ and Vertical Mapper™. Bedrock and surficial geologic mapping in Benton County is based on Allison (1953), Vokes and others (1954), Baldwin (1955), Bela (1979), Walker and Duncan (1989), Walker and MacLeod (1991), and O'Connor and others (2000). The western part of Benton County lies within the Coast Range and associated foothills, and comprises a thick sequence of Tertiary volcanic, sedimentary, and volcaniclastic rocks complicated by sills and dikes of basalt and gabbro (Figure 2). East of the Coast Range foothills lies the central Willamette Valley that has been infilled with unconsolidated Quaternary sediments. The sediments comprise channel and floodplain alluvium (Holocene), fine-grained Missoula Flood deposits (Pleistocene), fluvial sand and gravel deposits that predate the Missoula Floods of 12.7–15 ka, and older fine-grained Pleistocene alluvium (Figure 2).

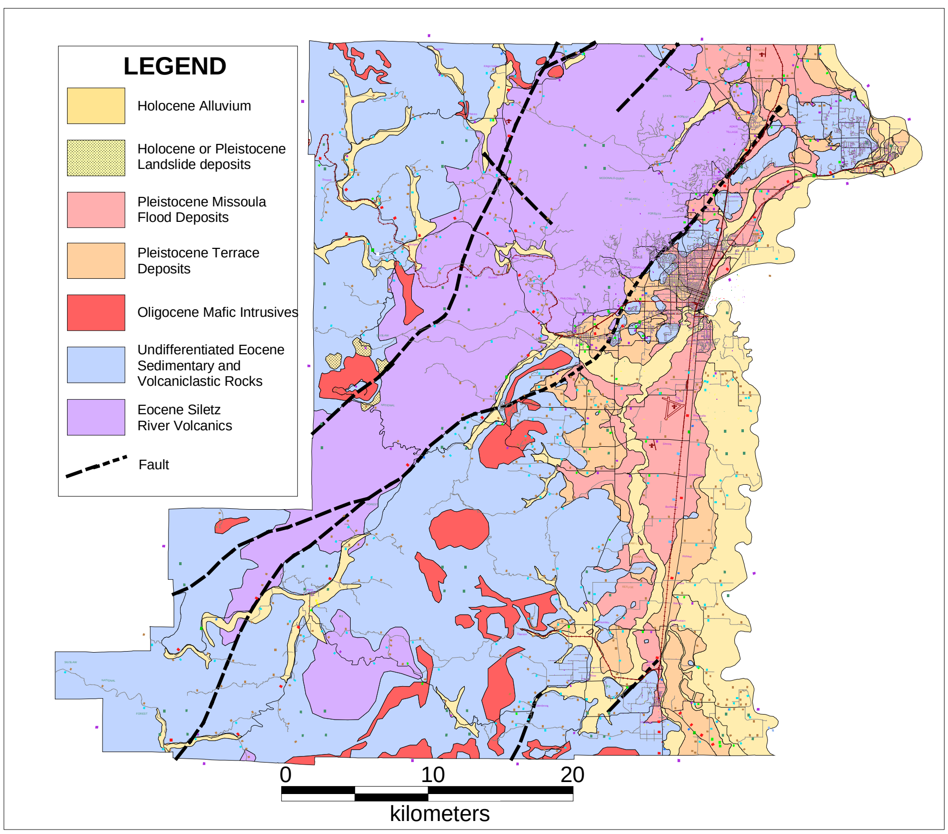

Figure 2. Generalized geologic map of Benton County.

Characterization of the distribution and thickness of soil units in the central Willamette Valley was accomplished using geologic maps, surface SH-wave refraction data, geotechnical subsurface investigations, and water-well data. Geotechnical investigations mainly conducted in the Corvallis area by the Oregon Department of Transportation (ODOT) and various private consulting firms were also utilized in this study. Water-well data were obtained from the Oregon Department of Water Resources (ODWR). Data from wells located by ODWR staff comprise the main basis for the geologic model, but these data were augmented with ODWR data from wells located only to the quarter-quarter section (Figure 3). SH-wave refraction techniques (Wang and others, 1998; Wang and others, 2000) were used to determine subsurface geologic materials and determine average shear-wave velocity for mapped stratigraphic units. SH-wave data were collected at 11 sites and largely focused around the Corvallis-Philomath urban areas (Figure 3). SH-wave data were processed on a personal computer using the commercial software package SIP by Rimrock Geophysics, Inc. (version 4.1, 1995). To process the data, refractions for each layer were identified, and then first-arrival times were picked and used to generate a shear-wave velocity model for the profile surveyed (see **Table** A-1 in Appendix A for a detailed shear-wave velocity profile at each site).

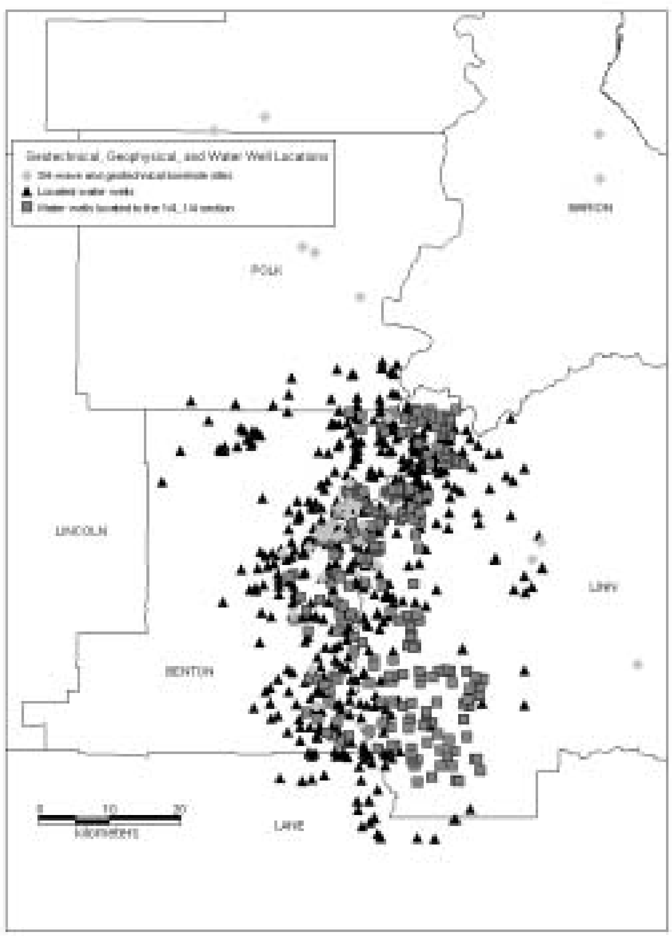

Figure 3. Location map of geotechnical boreholes, water well, and shear-wave sites used for the Benton County geologic model.

Ground shaking amplification

Soils and poorly consolidated sedimentary rocks overlying bedrock near the surface can modify bedrock ground shaking caused by an earthquake. The physical properties, spatial distribution, and thickness of geologic materials above bedrock can influence the strength of shaking by increasing or decreasing it and/or by changing the frequency of shaking. The method used to evaluate these modifications was developed by the Federal Emergency Management Agency (FEMA) (Building Seismic Safety Council, 1994). This method was adopted in the 1997 version of the Uniform Building Code (International Conference of Building Officials [ICBO], 1997) and will henceforth be referred to as the UBC-97 methodology. This 1997 version of the Uniform Building Code was adopted by the State of Oregon in October 1998 and became the *State of Oregon 1998 edition Structural Specialty Code*.

The UBC-97 methodology defines six soil categories that are based on average shear-wave velocity, Standard Penetration Test (SPT) value, or undrained shear strength in the upper 100 ft (30 m) of the soil column (Table 3). The six soil categories are Hard Rock (A), Rock (B), Very Dense Soil and Soft Rock (C), Stiff Soil (D), Soft Soil (E), and Special Soils (F). Category F soils are very soft soils that require site-specific evaluation. The ground motion amplification ranges from none (Hard Rock/A), to high (Soft Soil/E and F).

Table 1. UBC-97 Soil Profile Types **(ICBO, 1997).**

Soil Type	Soil Name	Average Soil Properties for Top 30 m (100 feet)		
		Shear-wave Velocity,Vs (m/s)	Standard Penetration Test, N (blows/foot)	Undrained Shear Strength s_u (kPa)
S_A	Hard Rock	>1,500	-	-
S_B	Rock	760 to 1,500		
S_C	Very Dense Soil and Soft Rock	360 to 760	>50	>100
S_D	Stiff Soil	180 to 360	15 to 50	50 to 100
S_E	Soft Soil	<180	<15	<50
S_F	Soil Requiring Site-specific Evaluation			

Utilizing the UBC-97 methodology, a ground motion amplification map for Benton County was generated (Map 1). The Quaternary stratigraphy of the central Willamette Valley in Benton County was differentiated into four main stratigraphic units: (1) Holocene channel and floodplain alluvium; (2) Pleistocene fine-grained flood deposits associated with the Missoula Floods of 15–12.7 ka; (3) Pleistocene sand and gravel deposits that predate the Missoula Flood deposits; and (4) Pleistocene fine-grained alluvium that predates all of those soils. These geologic units and their average shear-wave velocity and liquefaction susceptibility are listed in Table 2. Because SH-wave testing provided data for bedrock from only two sites, data from ten nearby sites reported in Wang and Madin (1999c, d) with bedrock units comparable to those exposed in Benton County were also used to determine the average shear-wave velocity for bedrock.

Table 2. Geologic units and their average shear-wave velocity (m/s), average standard penetration test value (N-count), and liquefaction susceptibility.

Age	Geologic Unit	Average Shear-Wave Velocity (m/s)	Average N-count (blows/foot)	Liquefaction susceptibility	O'Connor and others (2000) equivalent units
Holocene	Channel and floodplain alluvium	188	13	moderate to high	Qabs Qay Qal Qau
Pleistocene	Fine-grained Missoula Flood deposits	180	10	low	Qws
Pleistocene (pre-Missoula Floods)	Sand and gravel	509	22	low	Qg_2
Pleistocene	Fine-grained alluvium	371	21	low	--
Tertiary	Bedrock	822	--	none	--

The ground motion amplification map assigns UBC soil types, based on average shear-wave velocity for the upper 30 m of the soil column, to hazard categories as follows: (1) none (B type soil); (2) low (C type soil); and (3) moderate (D type soil) (Map 1). In general, the Coast Range and associated foothills have no ground motion amplification hazard reflecting bedrock exposures or a very thin mantle of soil overlying bedrock. Adjacent to the Coastal Range foothills lies a transitional zone characterized by a C type soil profile, where the majority of the upper 30 m of the section is comprised of bedrock, weathered rock, and stiff or very dense soils. On the east, toward the Willamette River, lies an area with a D type soil profile (moderate ground motion amplification hazard). The Corvallis-Philomath urban areas encompass all three ground motion amplification hazard zones. The purpose of this map is to convey general ground motion amplification in Benton County; the map is not intended to be used in place of site-specific studies. No A-type, E-type, or F-type soils are on the map because of data limitations and mapping scale. It is entirely possible that E-type and F-type soils exist within the study area, especially near streams and rivers in the Willamette Valley.

Liquefaction

Liquefaction is a phenomenon in which shaking of a saturated soil causes its material properties to change so that it behaves as a liquid. In qualitative terms, the cause of liquefaction was described very well by Seed and Idriss (1982): “If a saturated sand is subjected to ground vibrations, it tends to compact and decrease in volume; if drainage is unable to occur, the tendency to decrease in volume results in an increase in pore water pressure, and if the pore water pressure builds up to the point at which it is equal to the overburden pressure, the effective stress becomes zero, the sand loses its strength completely, and it develops a liquefied state."

Soils that liquefy tend to be young, loose, granular soils that are saturated with water (National Research Council, 1985). Unsaturated soils will not liquefy, but they may settle. If an earthquake induces liquefaction, several things can happen: (1) the liquefied layer and everything lying on top of it may move downslope; (2) the liquefied layer may oscillate with displacements large enough to rupture pipelines, move bridge abutments, or rupture building foundations; and (3) light objects, such as underground storage tanks, can float toward the surface, and heavy objects, such as buildings, can sink. Typical displacements can range from centimeters to meters. Thus, if the soil at a site liquefies, the total damage resulting from an earthquake can be dramatically increased from that caused by shaking alone.

Liquefaction hazard potential was first evaluated on the basis of age and engineering properties of the geologic unit and hydrologic conditions. Youd and Perkins (1978) found that the liquefaction potential for different sediments is related to age and depositional environment. Table 3 summarizes the liquefaction potential for several continental deposits (Youd and Perkins, 1978).

A further evaluation was performed for those geologic units with moderate to high liquefaction susceptibility and was based on the age and depositional environments in terms of ground shaking strength, SPT or shear-wave velocity, and the depth to water table (Seed and Idriss, 1971; Andrus and Stokoe, 1996). Andrus and Stokoe (1996) found that soils with a shear-wave velocity of less than 200 m/s have liquefaction potential. Hence, Holocene alluvium (V_s = 188 m/s) is considered to be the unit susceptible to liquefaction (Table 2).

Table 3. Estimated Susceptibility of Continental Deposits to Liquefaction (modified from Youd and Perkins, 1978).

Type of deposit	**Likelihood that Cohesionless Sediments, When Saturated, Would Be Susceptible to Liquefaction (by Age of Deposit)**			
	<500 yr	Holocene	Pleistocene	Pre-Pleistocene
River channel	Very high	High	Low	Very low
Flood Plain	High	Moderate	Low	Very low
Alluvial fan and Plain	Moderate	Low	Low	Very low
Lacustrine and playa	High	Moderate	Low	Very low
Colluvium	High	Moderate	Low	Very low
Talus	Low	Low	Very low	Very low
Tuff	Low	Low	Very low	Very low
Residual soils	Low	Low	Very low	Very low

Liquefaction hazard assignments for each geologic unit based on age, depositional environment, and average shear-wave velocity are listed in Table 2. The liquefaction potential hazard map for Benton County is illustrated on Map 2. As depicted on the map, areas with moderate to high liquefaction susceptibility, comprised of Holocene alluvium, are concentrated along the Willamette River, Coast Range tributaries, and major stream valleys within the Coast Range. Pleistocene terrace and Missoula Flood deposits were assigned a low liquefaction susceptibility hazard.

Earthquake-induced landslide

The earthquake-induced landslide hazard map is based on state-of-practice analysis for slope stability; empirical correlations of slope stability with engineering properties of materials; and the characterization of local topography, engineering geology, and hydrology with GIS tools.

Because failure mechanisms tend to vary with slope steepness, each grid cell was assigned to one of three slope categories, and different analytical techniques were applied to each category. Slopes between 0º and 10º were assigned a very low slope instability hazard because it was found that the slopes in this range have very low susceptibility for earthquake-induced failure (Jibson and others, 1998; McCrink and Real, 1996). Steep slopes (>25º), which most commonly fail by rock falls, rock slides, and debris slides (Keefer, 1984), are analyzed by means of an empirical relationship that relates slope stability to degree of weathering, strength of cementation, spacing and openness of rock fractures, and hydrologic conditions (Keefer, 1984, 1993). Moderate slopes (10º–25º) produce larger numbers of rotational slumps and translational block slides in soil (Keefer, 1984). Slopes between 10º and 25º were analyzed by means of a slope stability analysis based on slope inclination, engineering properties of soil units, and hydrologic conditions.

Existing Landslides

Motion of existing landslides is highly variable, ranging from active movement to stable. Although most earthquake-induced landslides occur in materials not previously involved in sliding (Keefer, 1984), it requires site-specific studies to understand the nature of any existing landslide. Therefore it was assumed that the slip planes of mapped landslides are at reduced shear strength of unknown value and that the slide masses are inherently unstable under earthquake loading. Existing landslides are conservatively assigned to the high hazard category, and no analytical techniques were applied. The mapping of existing landslides is described in detail in the ***Water-induced Landslide Hazard*** section.

Steep Slopes (>25º)

Slopes >25º are particularly vulnerable to bedrock failures. Keefer (1984, 1993) noted that more than 90 percent of earthquake-induced slope failures on rock slopes were rock falls and rock slides; typically thin, highly disrupted landslides that move at high velocities. The physical characteristics of the rock masses underlying steep slopes are of fundamental importance in evaluating their susceptibility to slope failure. Physical properties of rock that can be used as indicators of slope stability include degree of weathering, degree of induration, nature and spacing of fractures, and hydrologic conditions. Keefer (1993) developed a decision tree (Figure 4) to assess the earthquake hazard potential for steep slopes (>25º). The decision tree (Figure 4) was used as a reference guide to evaluate hazard potential on steep slopes (>25).

Previous geologic investigations (Vokes and others, 1954; Baldwin, 1955;Walker and Duncan, 1989; Bela, 1979) indicate that the rocks exposed in Benton County are typically intensely weathered and moderately to highly jointed. These factors coupled with prolonged saturated conditions during the winter months contribute significantly to a propensity for sliding. As a result, steep slopes (>25°) were assigned to a high relative hazard category. The potential ramifications associated with long-duration ground shaking from a Cascadia subduction earthquake (Clague and others, 2000) were also taken into consideration in the hazard assignment for steep slopes.

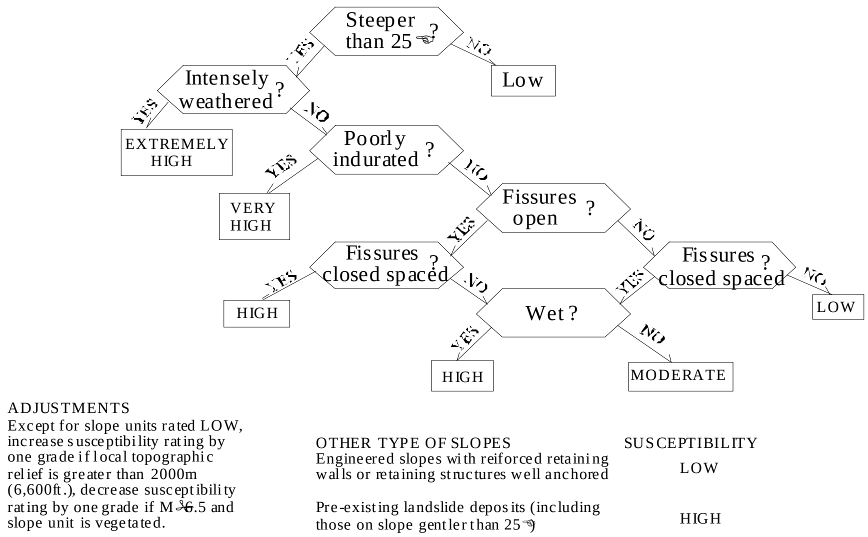

Figure 4. Decision tree for evaluation of earthquake-induced rock slope hazard (Keefer, 1993).

Moderate Slopes (10º to 25º)

The stability analysis for moderate slopes is based on the dynamic slope stability analysis of Newmark (1965) as verified and extended to regional-scale work by Wilson and Keefer (1983, 1985), Wieczorek and others (1985), Jibson (1993, 1996), and Jibson and Keefer (1993). The procedure to assign hazard categories takes several steps. First, using infinite slope analysis, the static factor of safety is calculated for each grid element. This factor of safety is then used to calculate the *critical acceleration*, which is the acceleration required to overcome friction and initiate sliding in the soil mass. The critical acceleration is then used in conjunction with earthquake input parameters to calculate the total displacement that is expected to occur during the design earthquake. This procedure has been used in Oregon by Black and others (2000a, b), Hofmeister and others (2000a, b), Wang and Wang (2000), and Wang and others (2001).

The *factor of safety (FS)* calculation for a static infinite slope model is discussed in detail in the next section entitled ***Water-induced Landslide Hazard***. The *critical acceleration* (a_c) in terms of g can be obtained through an equation developed by Newmark (1965):

$$a_c = (FS\text{-}1) \sin \alpha$$

where *FS* is the static factor of safety and α is the thrust angle.

Newmark displacement (D_N) is a function of critical acceleration and Arias Intensity according to the following empirical regression equation (Jibson, 1993):

$$\log D_N = 1.460 \log I_a - 6.642 a_c + 1.546$$

where I_a is the Arias Intensity in meters per second. The Arias Intensity (I_a) can be estimated by a relationship developed by Wilson and Keefer (1985):

$$\log I_a = \mathbf{M} - 2 \log R - 4.1$$

where **M** is the moment magnitude of a design earthquake and R is the earthquake source-to-site distance in kilometers. A M 8.5 subduction zone earthquake approximately 20 km offshore was used for slope stability analysis in this project. This is approximately equivalent to an Arias Intensity (I_a) of 3.9 m/s.

Finally, the total displacement was used to assign that element of slope to an earthquake-induced slope instability hazard category. Hazard categories used for this project were:

Low	Displacement <10 cm (3.9 in.)
Moderate	Displacement 10 -100 cm (3.9-39 in.)
High	Displacement > 100 cm (39 in.)

The results from the analyses for the three slope categories and the mapped landslide layer were combined to construct the earthquake-induced landslide hazard potential map for Benton County (Map 3).

WATER-INDUCED LANDSLIDE HAZARD

Common landslide triggers include intense rainfall, rapid snowmelt, water-level changes, volcanic eruptions, and strong ground shaking during earthquakes (National Research Council, 1996). In this study, we evaluated landslides that are triggered by water-related factors and delineate landslide susceptibility for Benton County at a regional scale (1:50,000 to 1:500,000) based on a landslide inventory and infinite slope modeling. This water-related landslide hazard differs from the earthquake-induced landslide hazard mainly in the type of failure and the triggering mechanism.

Landslide Inventory

The first part of the slope stability analysis performed as part of this investigation involved identifying existing landslides through aerial photo interpretation, available landslide data, and limited field investigations in the Corvallis area.

Benton County

Landslides mapped from previous investigations were digitized and utilized in this study. Bela (1979) mapped landslide deposits as part of an assessment of geologic hazards for eastern Benton County. Landslide deposits mapped by Bela (1979) at a scale of 1:24,000 in the Lewisburg, Corvallis, Greenberry, and Monroe 7.5' quadrangles were transferred by inspection from paper copies into MapInfo using 7.5' Digital Raster Graphic (DRG) topographic base maps. Additional landslide deposits, outside the above-mentioned 7.5' quadrangles, were mapped by Bela (1979) at a scale of 1:62,500. These slide deposits were also transferred by inspection to 7.5' DRG topographic base maps. However, it must be noted that the transfer of these landslide deposits was complicated by base maps at different horizontal scales (1:24,000 vs. 1:62,500) as well as various contour intervals.

Additional landslide deposits were compiled from the Salem 1° by 2° geologic quadrangle mapped by Walker and Duncan (1989); a digitized soil survey of the Alsea area by Corliss (1973); and a digitized database of slope failures compiled by Hofmeister (2000). In an effort to identify additional large, deep-seated landslides, aerial photo coverages for Benton County from 1948 (1:20,000), 1970 (1:20,000), and 1994 (1:24,000) were inspected using a stereo scopic viewers. Large areas interpreted to reflect slide deposits based on topographic/geomorphic expression were transferred directly into MapInfo with the use of Digital Raster Graphic (DRG) base maps. No efforts were made to field-check any of the potential landslide deposits mapped during this portion of the investigation.

Corvallis-Philomath Urban Areas

A more detailed slide map for within and surrounding the Corvallis-Philomath urban growth boundary was also compiled (Figure 5). Landslides were compiled from geologic mapping by Bela (1979), a digital soil map of the MacDonald-Dunn Research Forest, and exhaustive photogeologic mapping from aerial photos. Forest cover in the area makes it very difficult to see subtle landforms associated with landslides. In order to "see through" the trees, a time-series of photographs was examined, in hopes of catching most of the area without tree cover due to periodic logging or clearing for agriculture or development. Photo coverages of the area from 1936, 1944, 1948, 1956, 1963, 1970, 1978, 1990, and 1998 were examined in stereo, and any areas of slide topography were transferred by inspection to MapInfo, with Digital Orthophoto images as a base maps.

Very limited field checking was done for most of the larger slides within the urban area. The field checking was limited to driving through the affected areas, because most of the larger slides are on private property, and there was not sufficient time to obtain permission to field-check offroad areas. The larger slides that are on the map are those for which plausible evidence of sliding was observed in the field check.

A total of 110 possible slides was mapped in the Corvallis-Philomath study area (Figure 5). The slides range in size from a fraction of an acre to over 50 acres, and most are outside the Corvallis and Philomath Urban Growth Boundaries. Figure 5 is a slope map of the study area derived from the 10-m Digital Elevation Model (DEM) resampled to 50 m. Clearly, mostof the steep slopes are in the hills surrounding the urban growth boundaries. Most of the smaller slides are likely to be debris flows or soil flows, involving rapid failure of saturated soil or colluvium. Most of the larger slides are likely to be deeper seated rotational slumps or translational block slides, involving the movement of soil, colluvium, and underlying bedrock. One particularly notable slide complex occurs at Vineyard Mountain, at the north end of the study area. Bela (1979) shows some large slide areas here, and numerous small shallow slides were reported and investigated in conjunction with development of the area. This geotechnical study concluded that the abundant small slides in the area were occurring in thin deposits of soil and colluvium. Inspection of the historic air photos in this study suggests that these small slides were occurring on a much larger, deep-seated bedrock slide mass.

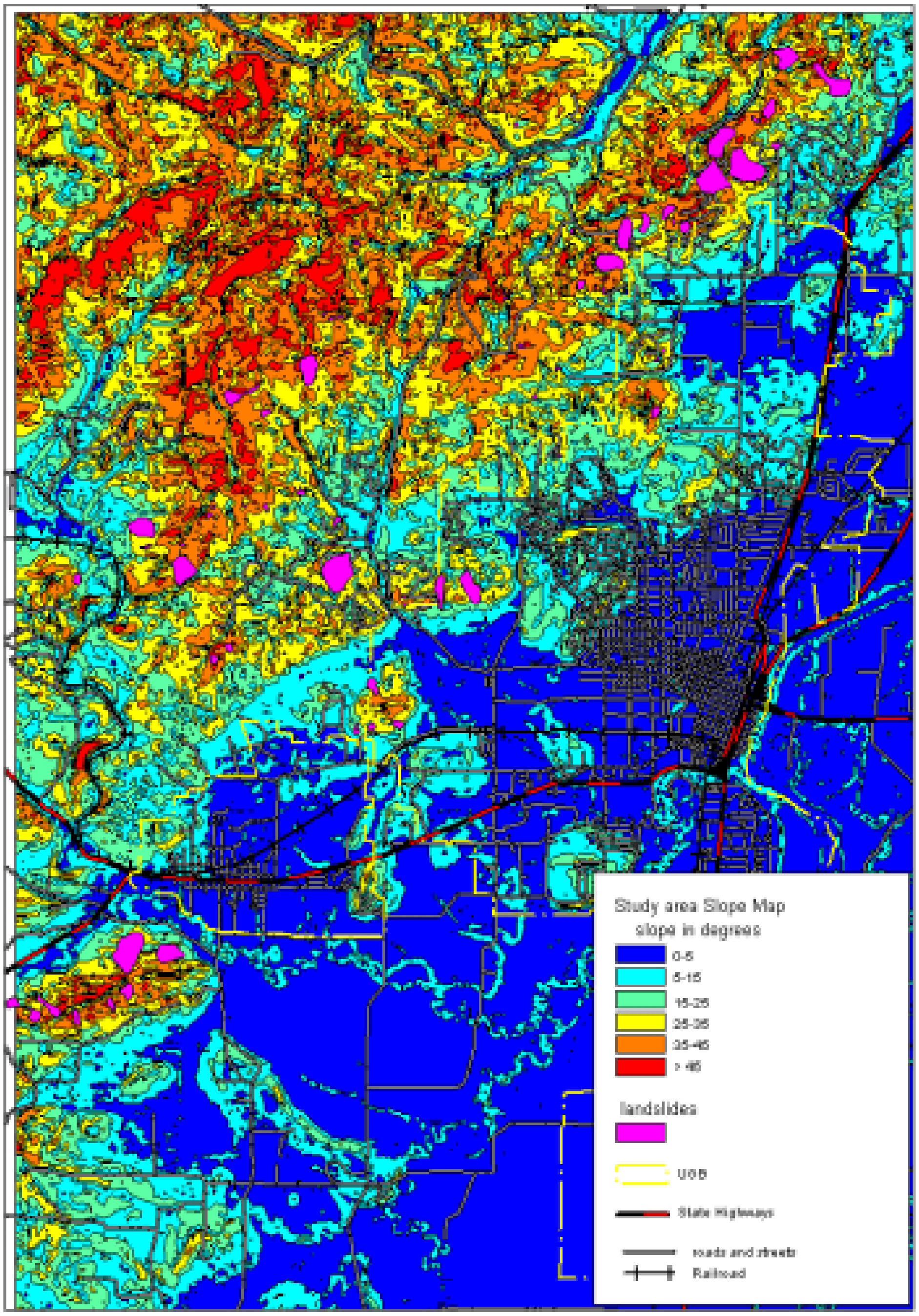

Figure 5. Slope map of the Corvallis-Philomath Urban Growth Boundaries and surrounding area with mapped landslide deposits.

Limitations

There are several significant limitations to both the countywide landslide inventory and the more detailed inventory of the Corvallis-Philomath urban area . First, for many slides, extensive field checking should be done to confirm the presence of a slide. Second, many parts of the area were forested during the entire span covered by the photo time series. It was not possible, within the scope of this project, to map the areas where forest cover may significantly obscure the features. Hence, many areas without mapped slides may indeed have slides that were not visible given the methods of this report. There was also no effort made to distinguish between the types of slides mapped. This is important, because in the case of debris flows, the hazard is likely to be in the runout zone, with lesser hazard in the area from which the slide originates. In the case of deep-seated slides, there may be less risk of rapid, life-threatening motion but a high risk of slow movement with incremental damage to structures.

Model Analysis

The factor of safety (*FS*) for an infinite slope in material having both frictional and cohesive strength is given by:

$$FS = \frac{c + \sigma' \cos\theta \tan\phi}{\sigma \sin\theta}$$

where c — soil cohesion
σ' — effective normal stress
θ — slope angle
ϕ — soil friction angle
σ — total normal stress

To implement the slope stability analysis, we used the GIS programs MapInfo and Vertical Mapper. A Digital Elevation Model (DEM) for Benton County with a 10-m grid spacing was acquired from the U.S. Geological Survey (USGS). Vertical Mapper was used to calculate slope angle for each grid cell from the USGS DEM. Digitized soil maps and relational soil property databases for the Benton County area (Knezevich, 1975), Alsea area (Corliss, 1973), Lane County (Patching, 1987), and Linn County (Langridge, 1987) were obtained from the National Resource Conservation Service (NRCS) through a SSURGO data download.

The factor of safety calculation specifically requires slope angle, depth to the failure plane, thickness of soil mass, unit weights for each soil layer, porosity for each soil layer, depth to the ground water table, and material strength properties (cohesion and internal friction angle) along the basal failure plane. Slope angle was calculated using Vertical Mapper with the 10-m DEM and the output values were stored at the same 10-m grid spacing as the DEM. The remainder of the input parameters were grouped according to soil polygon boundaries, using engineering properties contained in the NRCS relational soil databases. In particular, the relational soil databases contain information on Unified Soil Classification System (USCS) designation, bulk density, plasticity index, clay content, average thickness for each soil layer, and depth to bedrock for each soil unit if encountered in the depth of the soil survey. The data within the NRCS databases and the following assumptions were used for the calculation of the total and effective stresses for each soil unit (Black and others, 2000a and b; Hofmeister and others, 2000).

Depth to failure plane: The depth to failure plane was assumed to occur at the soil-bedrock interface if listed in the soils database. Depth to bedrock was listed in the NRCS database as a range, the lowest value of which was used in the stability analysis. If bedrock was not encountered during the depth of survey, the failure plane was assumed to be at a depth of 2.44 m (8 ft).

Thickness of soil units:	Where bedrock was not encountered in the depth of the survey, the properties of the lowest reported soil layer were assumed to extend to the depth of the failure plane.
Density:	Soil densities were reported as a range of "moist bulk density." Given that the samples were collected during summer field work (U.S. Department of Agriculture, 1996) when the soils were thoroughly dried, it was assumed that the dry bulk density for factor-of-safety calculations was the average of the reported "moist bulk density" range.
Porosity:	Porosity values were assigned according to the dominant USCS soil type for each layer listed in the NRCS database. Values are listed in Table 4 and were largely inferred from charts listing typical soil index properties in Naval Facilities Engineering Command (NFEC) (1986).
Unit weight:	Unit weights were calculated assuming 100% saturation.
Depth to water table:	If the depth was not reported, the water table was assumed to be at the surface consistent with other assumptions of saturated conditions.

Soil strength properties were assigned according to the dominant USCS soil listed in the lowest layer of each map unit recorded in the NRCS databases. In the absence of laboratory data for specific soils and due to the highly variable nature of geologic materials, the cohesion values used for SM, ML, CL-ML, CL, MH, and CH soils are typical saturated values reported by Driscoll (1979) (Table 4). GW, GP, GM, GC, and SW soils were assigned a lower cohesion value of 2.5 kPa to account for apparent cohesion inferred from modeling trials, part of which may also reflect root strength. Friction angles were assigned on the basis of USCS classification according to typical strength properties listed in Driscoll (1979) and USDA (1981) (Table 4).

The input parameters for the factor-of-safety calculation were grouped according to soil polygon boundaries. Hence, each soil polygon has a unique identifier, a map unit symbol in this case, as well as values for total and effective stress, cohesion, and friction angle (Appendix A). The slope grid, with a 10-m spacing, was then updated with the total and effective stress, cohesion, and friction angle assigned to the soil polygon that the slope point falls within. As a result, all parameters necessary for the factor-of-safety calculation were stored in one database. The static factor of safety for each grid cell could then be calculated using standard MapInfo database capabilities.

Factors which control the distribution of slides

The nature of the material making up a slope is an important factor. The thickness and engineering properties of soil, colluvium, and weathered rock; shear strength and structure of the bedrock; and hydrologic conditions are also very important. In general it is very difficult and time consuming to map the thickness of soil and colluvium, but the thickness is typically greater in the bottoms of drainages than on open slopes or ridges. This is reflected in the relatively common association of slides with minor drainages.

Table 4. USCS soil type and assigned engineering properties.

USCS	Porosity (%)	Cohesion (kPa)	Effective Friction Angle (ϕ) (degrees)
GW	30	2.5	39
GP	30	2.5	38
GM	29	2.5	38
GC	26	2.5	39
SW	33	2.5	38
SM	35	20	34
ML	41	9	32
CL-ML	38	22	32
CL	42	13	28
MH	48	20	25
CH	59	11	19

Bedrock slides are likely to be controlled by the type of rock and its degree of weathering, and the presence and orientation of structures in the rock. For example, in the Corvallis-Philomath study area, the majority of slides occurs in areas mapped as Siletz River volcanic rocks. This is a unit of interbedded basalt lava flows and sedimentary beds of sandstone and mudstone. Although intact basalt flows are typically quite competent, the presence of weak sedimentary interbeds can make the unit as a whole quite susceptible to landslides. In addition, the basalt flows are typically quite permeable to groundwater, while the sediments are not, so that groundwater often perches on the sediment-basalt contact, leading to saturated conditions and subsequent weakening of the rock. Existing geologic mapping does not distinguish the basalt and sediment layers of the Siletz River volcanic rocks, but both Bela (1979) and the Vineyard Mountain landslide study stress the association of the Vineyard Mountain slides with the sedimentary interbeds. Sedimentary bedrock units, which are the predominant unit within the Urban Growth Boundary seem to be much less susceptible to slides, though this may in part be due to the fact that the slopes are generally less steep where the sedimentary units are present.

Structures in bedrock, such as faults and fractures, can influence landslide susceptibility by providing potential failure planes for sliding. The orientation of structures can be mapped to some extent. However, the orientation of the natural layering or bedding of the rock, particularly where sedimentary rock is interlayered with basalt, is more important. If the layers are tilted parallel to the slope (as is the case, e.g., at Vineyard Mountain), they are much more prone to slide. This situation is called a dip slope, and it may be possible to map areas that are likely to have this condition with existing geologic data and GIS techniques.

Bela (1979) noted the importance of another bedrock condition that results in landslide occurrence. Dikes and sills of basalt and gabbro, both relatively strong rock, are commonly found injected into mudstone and sandstone units (Eocene Tyee Formation) in the area. Slides commonly occur along the boundaries between these two rock types. The higher peaks within Benton County such as Marys Peak, Grass Mountain, and Flat Mountain are cored by the above-mentioned Oligocene intrusives. These peaks are commonly flanked by large, deep-seated landslide deposits most likely reflecting a propensity for sliding along the boundaries of intrusive bodies.

Landslide hazard assignment

The activity of existing landslides is extremely variable, ranging from active movement to stability. Site-specific investigations are required to characterize the nature of any existing landslide. The shear planes of mapped landslides are assumed to be at a reduced shear strength of unknown value. Consequently, existing landslides are conservatively assigned to a high hazard rating, and no analytical techniques were used for this portion of the slope stability analysis.

Table 5 was used to assign landslide hazard based on factor-of-safety values. The factor of safety is the ratio of the shear strength over the shear stress required for equilibrium of the slope. The required factor of safety is usually in the range of 1.25 to 1.5 for highway slope design (Abramson and others, 1996). The slope with a factor of safety less than 1.25 would likely fail. Therefore, high landslide hazard was assigned to the cells with a factor of safety less than 1.25.

Table 5. Landslide hazard assignments from factor of safety.

Factor-of-Safety Range	**Hazard Rating**
Greater than 3.0	Low
1.25–3.0	Moderate
Less than 1.25	High

The landslide hazard map (Map 4) is an overlay of the three hazard layers based on factor-of-safety values from modeling, and the existing landslide layer. The hazard map delineates areas of low, moderate, and high landslide susceptibility. However, it is important to note that the hazard assignments were based on limited data and computer modeling. Cautions need to be exercised in using the maps.

SEISMIC RISK ASSESSMENT

Sound earthquake risk reduction plans should imcorporate detailed risk assessment based on the best available data. DOGAMI completed a seismic risk assessment for the State of Oregon (Wang and Clark, 1999), utilizing the earthquake risk assessment software HAZUS97 from the Federal Emergency Management Agency (NIBS, 1997), and statewide hazard information (Wang and Clark, 1999). Preliminary seismic risk information for Benton County was included in the statewide risk assessment (Wang and Clark, 1999). The information used in these rough regional studies used the default building data in HAZUS97 and statewide seismic hazard data.

In this study, seismic risk assessment for Benton County was performed with the seismic hazard maps developed in this project and HAZUS99 software by FEMA (NIBS, 1999). We augmented the building inventory provided in HAZAUS99 for the county by extrapolating available building data from the city of Corvallis and Benton County and targeted field surveys (Rad and Hasenberg, 2000).

Building Inventory

The default building inventory of HAZUS99 was derived from a nationwide database analysis (NIBS 1999). However, this default inventory might not reflect the actual characteristics of building stock in Benton County. With support from DOGAMI, a detailed building survey was conducted in downtown Corvallis by Portland State University (PSU) (Rad and Hasenberg, 2000). The building inventory contained in HAZUS99 was augmented with survey data and available building information from various sources (Rad and Hasenberg, 2000). Rad and Hasenberg (2000) concluded that:

(1) Total single-family residential building area from the project data was 22% larger than the HAZUS default data. This is largely due to the fact that certain tracts are growing rapidly and the survey data were much more up to date than the HAZUS default data.

(2) Building quantities for the Oregon State University campus were greatly underestimated in the HAZUS default data.

(3) The total commercial building areas are within 4% between the project data and HAZUS default data. However, the breakdowns into specific categories are very different. The project data show nearly twice as much retail commercial areas and about half as much office space as the HAZUS default data.

(4) Industrial buildings were underestimated by the HAZUS default data, largely due to expansion of the Hewlett Packard Company, Inc., campus.

The HAZUS99 default data (FEMA, 1999) categorized the buildings in Benton County into the “low code” seismic code category with data in both the “to code” and “inferior to code” divisions. For the mapping schemes developed in this study, buildings built prior to 1975 were put in the “low code – inferior” category and buildings built in 1975 and later were put in the “moderate code – to code” category. Oregon has been in seismic zone 2 or greater since 1975.

The augmented building inventory in Benton County contains 16 census tracts, over 26,256 households with a total population of about 70,811 (1990 Census Bureau data), about 21,000 buildings with a total square footage of about 67 million, and a building replacement value of $3.69 billion (1994 dollars). Table 6 lists the building counts in different occupancy classes and building types. A detailed building inventory is presented in Appendix B.

Table 6. Building counts in different occupancy classes and building type in Benton County.

Occupancy Classes		Building Type	
Class	**Count**	**Type**	**Count**
Residential	19,096	Wood	17,050
Commercial	772	Steel	457
Industrial	134	Concrete	291
Agriculture	653	Precast Concrete	266
Religion	73	Reinforced Masonry	389
Government	67	Unreinforced Masonry	290
Education	198	Mobile Homes	2,249
Total	**20,993**	**Total**	**20,992**

Essential and Lifeline Inventories

HAZUS99 also contains essential and lifeline inventories (Tables 7 and 8). These inventories were used in seismic risk assessment.

Table 7. Essential Facility Inventory

Hospitals	2 (124 beds)
Schools	31
Fire Stations	6
Police Stations	6
Emergency Operation	1

Table 8. Transportation System Lifeline Inventory

System	**Component**	**#Locations/ segments**	**Replacement Value (millions of dollars)**
Highway	Major Roads	30	1,730
	Bridges	24	60
	Tunnels	0	0
		Subtotal	1,790
Railways	Rail Tracks	41	211
	Bridges	0	0
	Tunnels	0	0
	Facilities	0	0
		Subtotal	211
Port	Facilities	0	0
Airport	Facilities	7	50
	Runways	7	196
		Subtotal	246
TOTAL			**2,247**

Input Seismic Hazards

HAZUS aggregates building data in a census tract and analyzes it at the centroid of the tract. To determine the hazard parameters in a particular tract, HAZUS overlays the hazard maps and the tract and takes hazard parameters at the centroid of the tract. However, this simple overlay may not accurately reflect the hazard level of a census tract. For this reason, the input seismic hazard parameters (ground motion amplification, liquefaction, and earthquake-induced slope failure) in each census tract (Table 9) were determined by visual comparison of overlays of the hazard maps, USGS quadrangle maps, zoning maps, and census tracts.

Table 9. Hazard parameters in each census tract used in the HAZUS analysis.

Census Tract	Soil Type	Landslide Hazard	Liquefaction Hazard	Water Table Depth (ft)
41003010200	B	Moderate	Very Low	0
41003000300	B	Moderate	Very Low	0
41003010300	B	Moderate	Very Low	0
41003010400	C	Moderate	Moderate	0
41003010500	B	Low	Low	0
41003000700	D	Low	Moderate	0
41003000100	D	Low	Moderate	0
41003000200	C	Low	Moderate	0
41003000400	B	Low	Very Low	0
41003000500	C	Low	Low	0
41003000600	D	Low	High	0
41003000800	D	Low	Moderate	0
41003000900	B	Low	Very Low	0
41003001000	C	Low	Moderate	0
41003001100	D	Low	Moderate	0
41003010100	C	Low	Moderate	0

Building damage due to liquefaction and earthquake-induced landslides is modeled in HAZUS as a permanent ground displacement. Census tracts with a liquefaction potential range from 2% of the developed land in a low-potential area to 25% in a high-potential area. The program checks to see if the threshold magnitude for the potential has been reached. The threshold magnitude depends on the potential category and the water-table depth. If the threshold magnitude has been reached for the tract, then HAZUS adds buildings to the “extensive” and “complete damage” categories. The program treats earthquake-induced landslides in the same way as liquefaction. Unfortunately, in HAZUS it is not possible to model loss of life that may occur if a catastrophic landslide or liquefaction occurs.

Earthquake Scenario

In Benton County, there are no active faults that have been identified to be significant earthquake sources. The Corvallis fault was mapped as a late Quaternary fault, and there is no evidence for late Pleistocene or Holocene displacement on the fault (Goldfinger, 1990; Yeats and others, 1991; Geomatrix, 1995). The ground shaking hazards that could significantly affect the county are from sources outside the county, especially from the Cascadia subduction zone. Although the probability of activity on the Corvallis fault is not clear, perhaps very low, a scenario of M 6.5 with focal depth of 10 km along the fault was modeled in this study. Another earthquake scenario is the probabilistic ground shaking hazard with a 500-year return period of Frankel and others (1997) (Figure 1). This scenario represents a ground shaking level similar to a M 8.5–9.0 Cascadia subduction earthquake 20 km off the Oregon coast (Wang and others, 2001).

Damage and Loss Estimates

1. Corvallis fault M 6.5 Scenario

The damage and loss estimates from the Corvallis Fault M 6.5 scenario are summarized in Table 10. The model predicts at least slight damage to about 10,578 buildings, with losses on the order of $707 million. Damages and losses are detailed in Appendix C.

Table 10. Summary of damage and loss estimates from Corvallis fault scenario.

	Damage Level	**Residential**	**Total**	
Building Damaged	Slight	5,401	5,771	
	Moderate	3,098	3,584	
	Extensive	807	1,060	
	Complete	113	163	
	Total	9,419	10,578	
Casualties	Severity 1 (Medical treatment without hospitalization)	2 a.m.	2 p.m.	5 p.m.
		48	110	56
	Severity 2 (Hospitalization but not life threatening)	7	19	10
	Severity 3 (Hospitalization and life threatening)	0	2	2
	Severity 4 (Fatalities)	0	2	1
Shelter	Displaced Households (# households)	695		
	Short Term Shelter (# people)	659		
Economic Loss	Property Damage losses ($millions)	520.2		
	Business Interruption losses ($millions)	187.1		
	Total ($ millions)	707.3		

The model predicts that only 56% of needed hospital beds would be available on the day following the scenario earthquake on the Corvallis fault; 71% of the beds will be back in service after one week, and 89% will be operational within 30 days. Predicted to be functioning on the day following the scenario earthquake are 37% of the emergency facilities, 34% of the schools, and 74% of the communication facilities . The model also predicts that five of the highway bridges will have a functionality of less than 90% on day 1, one of the bridges suffering at least moderate damage. The roads, railways, and runways are expected to remain fully functional. However, permanent ground displacements in areas of liquefaction hazards and landslides blocking highways are likely to occur.

2. 500-year Probabilistic Ground Shaking Scenario

The damage and loss estimates from the scenario are summarized in Table 11. The model predicts at least slight damage to about 11,270 buildings, with losses on the order of $976 million. Damages and losses are detailed in Appendix C.

Table 11. Summary of damage and loss estimates from the 500-year scenario.

	Damage Level	**Residential**	**Total**	
Building Damaged	Slight	5,646	6,008	
	Moderate	3,034	3,530	
	Extensive	759	1,066	
	Complete	464	666	
	Total	9,903	11,270	
Casualties		2 a.m.	2 p.m.	5 p.m.
	Severity 1 (Medical treatment without hospitalization)	89	266	126
	Severity 2 (Hospitalization but not life threatening)	15	50	23
	Severity 3 (Hospitalization and life threatening)	1	6	3
	Severity 4 (Fatalities)	1	6	3
Shelter	Displaced Households (# households)	994		
	Short Term Shelter (# people)	911		
Economic Loss	Property Damage losses ($millions)	700		
	Business Interruption losses ($millions)	275.8		
	Total ($ millions)	975.8		

HAZUS analyses predict that only 42% of needed hospital beds would be available on the day following the scenario earthquake; 57% of the beds will be back in service after one week, and 79% will be operational within 30 days. 34% of the emergency facilities, 33% of the schools, and 80% of the communication facilities are predicted to be functioning on the day following the scenario. The model also predicts that five of the highway bridges have a functionality of less than 90% on day 1, one of the bridges suffering at least moderate damage. The roads, railways, and runways are expected to remain fully functional. However, permanent ground displacements in areas of liquefaction hazards and landslides blocking highways are likely to occur.

Casualty results in HAZUS are based on injuries and deaths from building damage and bridge damage only. Not included in the estimate are injuries and deaths resulting from fires following the earthquake, tsunamis, landslides, dam failures, or a release of toxic materials. As these can be major contributors to casualties, caution must be used in interpreting the HAZUS results. The functions used to compute the building and bridge casualties are also based on available historical data, which according to the HAZUS User's Manual are "not of the best quality." Data for developing such functions are usually gathered long after the earthquake occurs, and the level of detail is low. Casualty figures computed in HAZUS are given for 2 p.m., 2 a.m., and 5 p.m. events, as the distribution of population in various building-occupancy categories and on the highways depends on the time of day. Population exposure is computed, and then the casualty functions are engaged based on percentage of buildings in each of the damage states.

CONCLUSIONS

Great Cascadia subduction zone earthquakes have occurred many times in the past along the Pacific Northwest coast, the most recent one on January 26, 1700 (Clague and others, 2000). Future subduction zone earthquakes pose great seismic hazards and risk to Benton County. Strong ground shaking from the subduction zone earthquakes will likely last three minutes or more and be dominated by long-period ground motions (Clague and others, 2000). This long-period and long-duration ground shaking will cause widespread ground failures. The ground shaking hazard from the Cascadia subduction earthquakes and other sources has been assessed and is available in such publications as DOGAMI map GMS-100 (Madin and Mabey, 1996) and the probabilistic hazard maps of the United States Geological Survey (USGS) (Frankel and others, 1997). These maps provide a general seismic hazard level from all seismic sources. The ground motion design level in the *State of Oregon 1998 Structural Specialty Code* (Oregon Building Codes Division, 1998) is based on these probabilistic seismic hazard assessments.

However, the earthquake hazard is also affected by local surface and subsurface geologic, hydrologic, and topographic conditions, which allow the differentiation of *relative earthquake hazards*. We assessed these relative hazards in Benton County utilizing the best available geological, geotechnical, and water-well data, as well as limited field investigations. The maps show that the areas with high ground amplification and liquefaction hazards are concentrated along the Willamette River, while the areas with high earthquake-induced landslide hazard are spread out over the western part of the county in the Coast Range.

Oregon is prone to landslide hazards (Beaulieu, 1976), especially in the western part of the state, where steep slopes and conducive geological conditions are combined with abundant precipitation (Burns, 1998a). In Benton County, we delineated landslide hazard using a combination of landslide inventory and computer modeling based on the best available topographic, geologic, and soil data. The results show that Benton County has a low landslide hazard in the eastern part, low to moderate landslide hazard in the northwestern part, and moderate to high landslide hazard in the southwestern part of the county.

A detailed building survey was conducted for 90 percent of the commercial buildings in downtown Corvallis. The survey data, along with the available data from the City of Corvallis, Benton County, and other sources, were analyzed to augment the building inventory provided in HAZUS99. The analysis shows:

(1) Total single-family residential building area from the project data was 22% larger than the HAZUS default data. This is largely due to the fact that certain tracts are growing rapidly, and the survey data are much more up to date than the HAZUS default data.

(2) Building quantities for the Oregon State University campus were greatly underestimated in the HAZUS default data.

(3) The projected data and HAZUS default data have the same total area for commercial buildings, although the breakdowns into specific categories are very different. The projected data show nearly twice as much retail

commercial areas and about half as much office space as the HAZUS default data.

(4) Industrial buildings were underestimated by the HAZUS default data, largely due to the fact that the Hewlett Packard Company, Inc., campus was underestimated.

The relative seismic hazard maps, augmented building inventory, and other inventories provided in HAZUS99 were used to assess seismic risks in the county for two scenarios: (1) a M 6.5 earthquake on the Corvallis fault and (2) a probabilistic ground motion with 500-year recurrence interval (Frankel and others, 1997), which is similar to the ground shaking level generated by a M 8.5–9.0 Cascadia subduction zone earthquake 20 km offshore. The results indicate that the damage and losses from the scenarios would be devastating. A M 6.5 earthquake on the Corvallis fault at a depth of 10 km would cause at least slight damage to 10,578 buildings, about one hundred injuries and deaths, and approximately $707 million in losses. The 500-year probabilistic ground-shaking scenario would likely cause at least slight damage to 11,270 buildings, more than one hundred injuries and deaths, and approximately $976 million in losses.

DISCUSSION

Hazard Maps

The *Relative Earthquake Hazard Maps,* including ground motion amplification, liquefaction, and earthquake-induced landslide hazards, and the *Water-induced Landslide Hazard Map* for Benton County were developed based on local geologic, topographic, and hydrologic conditions. The local geologic conditions, including thickness and engineering properties of geologic materials, were derived from existing geological, geotechnical, topographic, and water-well data and limited field investigations. These data we used to construct three-dimensional geologic models, using the GIS software MapInfo™ and Vertical Mapper™. According to the scope of this project, most of the field investigations were concentrated in the Corvallis area (Corvallis-Philomath urban area). Consequently, a better geologic model and landslide inventory for that area was obtained. Nevertheless, the maps are all at a regional scale, not suitable for site-specific evaluations.

We derived the ground motion amplification hazard from a three-dimensional geologic model, using GIS software to assign hazard values on the basis of the UBC-97 methodology. Liquefaction hazard was derived in a similar manner, by use of the age and depositional environment of the geologic units and a simplified state-of-practice engineering analysis. Earthquake-induced and water-induced landslide hazards were analyzed with infinite-slope modeling and with the assumption of the worst hydrologic conditions: 100% saturation or 0 m groundwater table.

The relative earthquake hazard maps and water-induced landslide hazard map delineate those areas most likely to experience damage during a strong earthquake or heavy rainfall. This information can be used to develop a variety of hazard mitigation strategies such as the following:

Emergency response and hazard mitigation

One of the key uses of these maps is to develop emergency response plans. The areas indicated as having a higher hazard would be the areas where the greatest and most abundant damage will tend to occur. Planning for disaster response will be enhanced by the use of these maps to identify which resources and transportation routes are likely to be damaged.

Land use planning

The location of future urban expansion or intensified development should also consider earthquake and landslide hazards. Requirements placed on development could be based on the hazard zone in which the development is located. For example, the type of site-specific hazard investigation that is required for a particular location could be based on the maps.

Lifelines

Lifelines include road and access systems such as railroads, airports, and runways, bridges, and over- and underpasses, as well as utilities and distribution systems. The relative earthquake and landslide hazard maps are especially useful for estimation and mitigation of expected-damage to lifelines. Lifelines are usually distributed widely and often require regional as opposed to site-specific hazard assessments. The hazard maps presented here allow quantitative estimates of the hazard throughout a lifeline system. This information can be used for assessing vulnerability as well as deciding on priorities and approaches for mitigation.

Engineering

The hazard zones shown on the *Hazard Maps* **should not** serve as a substitute for site-specific evaluations based on subsurface information gathered at a site. The calculated values of the individual map may, however, be used to good purpose in the absence of such site-specific information, for instance, at the feasibility-study or preliminary-design stage. In most cases, the quantitative values calculated for these maps would be superior to a qualitative estimate based solely on lithology or non-site-specific information.

It is very important to recognize the limitations of these *hazard maps*, which in no way include information with regard to the probability of damage to occur. Rather, they show that when strong ground shaking or heavy rainfall occurs, the damage is more likely to occur, or be more severe, in the higher hazard areas. However, the higher hazard areas should not necessarily be viewed as unsafe. These limitations result from the nature of regional mapping, data limitations, and computer modeling.

Risk Assessment

HAZUS99 was developed by FEMA and the National Institute of Building Sciences (NIBS) as a tool for developing reliable earthquake damage and loss estimates that are essential to decision-making at the local, regional, state, and national levels of government. HAZUS99 contains a huge default database, ranging from building stock and lifeline facilities to fragility functions and was developed from available data nationwide. Some default data may not reflect the reality in Benton County. In this study, some effort was made to improve building data by extrapolating the sample building survey and available information from the City of Corvallis, Benton County, and other sources.

The risk assessment performed in this study can provide the basis for developing mitigation policy, for developing and testing emergency preparedness and response plans, and for planning for postdisaster relief and recovery. However, caution must be exercised in using the risk information due to the uncertainty and data quality inherent in the

HAZUS99 program and associated databases, for example, the uncertainty of earthquake activity on Corvallis fault.

ACKNOWLEDGMENTS

This project was supported by a professional services agreement with Benton County and from resources of the Oregon Department of Geology and Mineral Industries. County funds were derived from the Project Impact program of the Federal Emergency Management Agency. Jon Hofmeister of DOGAMI contributed greatly to this project by sharing practical insight on GIS data conversion and manipulation and in-depth review of the report. Stephen Dickenson and his students at Oregon State University provided geotechnical data and shared their soil amplification map in Corvallis area. Carol Hasenberg of Portland State University provided many review comments on seismic risk assessment.

REFERENCES

Abramson, L.W., T.S. Lee, S. Sharma, and G.M. Boyce, 1996, Stability and Stabilization Methods, John Wiley & Sons, Inc, New York.

Allison, I.S., 1953, Geology of the Albany Quadrangle, Oregon: Oregon Department of Geology and Mineral Industries Bulletin 37, 18 p.

Andrus, R.D., and Stokoe, K.H., 1997, Liquefaction resistance based on shear wave velocity: Report to the NCEER Workshop on Evaluation of Liquefaction Resistance (9/18/97 version), Jan. 4-5, Salt Lake City, Utah.

Atwater, B.F., 1987, Evidence for great Holocene earthquakes along the outer coast of Washington state: Science, v. 236, p. 942-944.

Atwater, B.F., and Hemphill-Haley, E., 1997, Recurrence intervals for great earthquakes of the past 3,500 years at northeastern Willapa Bay, Washington: U.S. Geological Survey Professional Paper 1576, 108 p.

Baldwin, E.M., 1955, Geology of the Marys Peak and Alsea Quadrangles, Oregon: U.S. Geological Survey Oil and Gas Investigations Map OM-162, scale: 1:62500.

Beaulieu, J.D., 1973, Environmental geology of inland Tillamook and Clatsop Counties, Oregon: Oregon Department of Geology and Mineral Industries Bulletin 79, 65 p., map scale 1:62,500.

Beaulieu, J.D., 1976, Geologic Hazards in Oregon, Ore Bin, v. 38, no. 5, p 67-86.

Bela, J.L., 1979, Geologic Hazards of eastern Benton County, Oregon: Oregon Department of Geology and Mineral Industries Bulletin 98, 122 p.

Black, G.L., Wang, Z., Wiley, T.J., Wang, Y., and Keefer, D.K., 2000a, Relative earthquake hazards of the Eugene-Springfield metropolitan area, Lane County, Oregon: Oregon Department of Geology and Mineral Industries Interpretive Map Series IMS-14, 1:24,000.

Black, G.L., Wang, Z., and Priest, G.R., 2000b, Relative earthquake hazard map of the Klamath Falls metropolitan area, Klamath County, Oregon: Oregon Department of Geology and Mineral Industries Interpretive Map Series IMS-19, 1:24,000.

Bolt, B.A., 1993, Earthquakes: New York, W.H. Free man and Co., 331 p.

Building Seismic Safety Council, 1994, NEHERP recommended provisions for seismic regulations for new buildings, 1994 edition, Part 1: Provisions: Federal Emergency Management Agency Publication FEMA 222A / May 1995, 290 p.

Burns, S. F., 1998a, Landslide Hazards in Oregon, Environmental, Groundwater and

Engineering Geology, ed. By S. Burns, Star Publishing Company, Belmont, CA, p303-315.
Burns, S. F., 1998b, Landslides in the Portland Area resulting from the Storm of February, 1996, Environmental, Groundwater and, Engineering Geology, ed. By S. Burns, Star Publishing Company, Belmont, CA, p353-365.
Clague, J.J., Atwater, B.F., Wang, K., Wang, Y., and Wong, I., 2000, Program Summary and Abstracts, Penrose Conference 2000: Oregon Department of Geology and Mineral Industries Special Paper 33.
Corliss, J.F., 1973, Soil survey of Alsea area, Oregon: U.S. Department of Agriculture, Soil Conservation Service, 82 p.
Driscoll, D.D., 1979, Retaining wall design guide: Portland, Oregon, U.S. Department of Agriculture, Forest Service, Pacific Northwest Region.
Frankel, A., Mueller, C., Barnhard, T., Perkins, D., Leyendecker, E. V., Dickman, N., Hanson, S., and Hopper, M., 1997, National 1996 Seismic Hazard Maps: U.S. Geological Survey, Open-File Report 97-131.
Geomatrix Consultants, Inc., 1995, Seismic design mapping, State of Oregon: Final report to Oregon Department of Transportation, Project no. 2442, var. pag.
Goldfinger, C., 1990, Evolution of the Corvallis Fault and Implications for the Oregon Coast Range, MS Thesis, Oregon State University, Corvallis, Oregon, 118p.
Harvey, A.F. and G.L. Peterson, 1998, Water-Induced Landslide Hazards: Western Portion of the Salem Hills, Marion County, Oregon, Oregon Department of Geology and Mineral Industries Interpretive Map Series IMS-6.
Harvey, A.F. and G.L. Peterson, 2000, Water-Induced Landslide Hazards: Eastern Portion of the Eola Hills, Polk County, Oregon, Oregon Department of Geology and Mineral Industries Interpretive Map Series IMS-5.
Heaton, T.H., and Hartzell, S.H., 1987, Earthquake hazards on the Cascadia subduction zone: Science, v. 236, p. 162–168.
Hofmeister, R.J., 2000, Slope failures in Oregon: GIS inventory for three 1996/97 storm events: Oregon Department of Geology and Mineral Industries Special Paper 34, 20 p.
Hofmeister, R.J., Wang Y., Keefer D.K., 2000a, Earthquake-Induced Slope Instability: Relative Hazard Map Western Portion of the Salem Hills, Marion County, Oregon, Oregon Department of Geology and Mineral Industries Interpretive Map Series IMS-17.
Hofmeister, R.J., and Wang Y., 2000, Earthquake-Induced Slope Instability: Relative Hazard Map Western Portion of the Salem Hills, Marion County, Oregon, Oregon Department of Geology and Mineral Industries Interpretive Map Series IMS-18.
Hofmeister R.J., Wang, Y., and Keefer, D.K., 2000b, Earthquake-induced slope instability: methodology of relative hazard mapping, western portion of the Salem Hills, Marion County, Oregon: Oregon Department of Geology and Mineral Industries Special Paper 30, 73 p.
Holzer, T.H., 1994, Loma Prieta damage largely attributed to enhanced ground shaking: EOS, v. 75, no. 26, p. 299-301 [reprinted in Oregon Geology, v. 56, no. 5 (Sept. 1994, p. 111-113].
International Conference of Building Officials, 1997, 1997 Uniform building code, v. 2, Structural design provisions: International Conference of Building Officials, 492 p.
Jibson, R.W., 1993, Predicting earthquake-induced landslide deposits using Newmark's sliding block analysis: Washington, D.C., National Research Council

Transportation Research Record 1411, p. 9-17.
Jibson, R.W., 1996, Use of landslides for paleoseismic analysis: Engineering Geology, v. 43, p. 291-323.
Jibson, R.W., Harp, E.L., and Michael, J.A., 1998, A method for producing digital probabilistic seismic landslide hazard maps: an example from the Los Angeles, California, area: U.S. Geological Survey Open-file Report 98-113.
Jibson, R.W., and Keefer, D.K., 1993, Analysis of the seismic origin of landslides: Examples from the New Madrid seismic zone: Geological Society of America Bulletin, v. 105, p. 521-536.
Keefer, D.K., 1984, Landslides caused by earthquakes: Geological Society of America Bulletin, v. 95, p. 406-421.
Keefer, D.K., 1993, The susceptibility of rock slopes to earth-quake induced failure: Association of Engineering Geologists Bulletin, v. 30, p. 353-361.
Keefer, D.K., and Schuster, R.L., 1993, A method for predicting slope instability for earthquake hazard maps, preliminary report: Association of Engineering Geologists Special Publication 10, p. 39-52.
Knezevich, C.A., 1975, Soil survey of Benton County area, Oregon: U.S. Department of Agriculture, Soil Conservation Service, 119 p.
Langridge, R.W., 1987, Soil survey of the Linn County area, Oregon: U.S. Department of Agriculture, Soil Conservation Service, 344 p.
Mabey, M.A., Madin, I.P., and Meier, D.B., 1995a, Relative earthquake hazard map of the Beaverton quadrangle, Washington County, Oregon: Oregon Department of Geology and Mineral Industries Geologic Map Series GMS-90.
Mabey, M.A., Madin, I.P., and Meier, D.B., 1995b, Relative earthquake hazard map of the Lake Oswego quadrangle, Clackamas, Multnomah, and Washington Counties, Oregon: Oregon Department of Geology and Mineral Industries Geologic Map Series GMS-91.
Mabey, M.A., Madin, I.P., and Meier, D.B., 1995c, Relative earthquake hazard map of the Gladstone quadrangle, Clackamas and Multnomah Counties, Oregon: Oregon Department of Geology and Mineral Industries Geologic Map Series GMS-92.
Mabey, M.A., Madin, I.P., Meier, D.B., and Palmer, S.P., 1995d, Relative earthquake hazard map of the Mount Tabor quadrangle, Multnomah County, Oregon: Oregon Department of Geology and Min eral Industries Geological Map Series GMS–89.
Madin, I.P., Priest, G.R., Mabey, M.A., Malone, S., Yelin, T.S., Meier, D., 1993, March 23, 1993, Scotts Mills earthquake-western Oregon's wake-up call: Oregon Geology, v. 55, no. 3, p. 51-57.
Madin, I.P., and Mabey, M.A., 1996, Earthquake hazard maps for Oregon: Oregon Department of Geology and Mineral Industries Geologic Map Series GMS-100.
Madin, I.P., and Wang, Z., 1999a, Relative earthquake hazard maps for selected urban areas in western Oregon: Astoria-Warrentown, Brookings, Coquille, Florence-Dunes City, Lincoln City, Newport, Reedsport-Winchester Bay, Seaside-Gearhart-Cannon Beach, Tillamook: Oregon Department of Geology and Mineral Industries Interpretive Map Series IMS-10.
Madin, I.P., and Wang, Z., 1999b, Relative earthquake hazard maps for selected urban areas in western Oregon: Ashland, Cottage Grove, Grants Pass, Roseburg, Sutherlin-Oakland: Oregon Department of Geology and Mineral Industries Interpretive Map Series IMS-9.
Madin, I.P., and Wang, Z., 1999c, Relative earthquake hazard maps for selected urban

areas in western Oregon: Canby-Barlow-Aurora, Lebanon, Silverton-Mount Angel, Stayton-Sublimity-Aumsville, Sweet Home, Woodburn-Hubbard: Oregon Department of Geology and Mineral Industries Interpretive Map Series IMS-8.

Madin, I.P., and Wang, Z., 1999d, Relative earthquake hazard maps for selected urban areas in western Oregon: Dallas, Hood River, McMinnville-Dayton-LaFayette, Monmouth-Independence, Newberg-Dundee, Sandy, Sheridan-Willamina, St. Helens-Columbia City-Scappoose: Oregon Department of Geology and Mineral Industries Interpretive Map Series IMS-7.

McCrink, T.P., and Real, C.R., 1996, Evaluation of the Newmark method for mapping earthquake-induced landslide hazards in the Laurel 7.5’ quadrangle, Santa Cruz County, California: Final Technical Report, California Department Conservation, Division of Mines and Geology.

National Institute of Building Sciences (NIBS), 1997, HAZUS, earthquake loss estimation methodology, prepared for the Federal Emergency Management Agency (FEMA): NIBS Documents 5200 (user's manual) and 5201-5203 (technical manual, 3 vols.). var. pag.

National Institute of Building Sciences (NIBS), 1999, HAZUS, FEMA's tool for estimating potential losses from natural disasters: Available on CD-ROM disks from National Institute of Building Sciences 1090 Vermont Avenue, NW, Suite 700 Washington, DC, 20005-4905, phone (202) 289-7800, fax (202) 289-1092, e-mail hazus@nibs.org. Internet http://www .fema.gov/HAZUS/

National Research Council, Commission on Engineering and Technical Systems, Committee on Earthquake Engineering, 1985, Liquefaction of soils during Earthquakes: Washington, D.C., National Academy Press, 240 p.

National Research Council, Transportation Research Board, 1996, Landslides Investigation and Mitigation, Special Report 247, ed. By K. Turner and R.L. Schuster, p673.

Naval Facilities Engineering Command (NFEC), 1986, Soil mechanics: Naval Facilities Engineering Command Design Manual 7.01, 348 p.

Newmark, N.M., 1965, Effects of earthquakes on dams and embankments: Geotechnique, v. 15, p. 139-159.

O’Connor, J.E., Sarna-Wojcicki, A.M., Wozniak, K.C., Polette, D.J., and Fleck, R.J., 2000, Origin, extent, and thickness of Quaternary geologic units in the Willamette Valley, Oregon: U.S. Geological Survey Professional Paper 1620, 52 p.

Patching, W.R., 1987, Soil survey of Lane County area, Oregon: U.S. Department of Agriculture, Soil Conservation Service, 369 p.

Rad, F.N. Rad, C.S. Hasenberg, 2000, Building Inventory Analysis for Benton County, Oregon, Department of Civil Engineering, Portland State University, 23p.

Schlicker, H.G., Deacon, R.J., Beaulieu, J.D., and Olcott, G.W., 1972, Environmental geology of the coastal region of Tillamook and Clatsop Counties, Oregon: Oregon Department of Geology and Mineral Industries Bulletin 74, 164 p.

Seed, H.B., and Idriss, I.M., 1971, Simplified Procedure for Evaluation Soil Liquefaction Potential, Journal of the Soil Mechanics and Foundation Division, ASCE, Vol. 97, SM9, p1249-1273.

Seed, H.B., and Idriss, I.M., 1982, Ground motions and soil liquefaction during earthquakes: Earthquake Engineering Institute Monograph Series, 134 p.

Seed, H.B., Romo, M.P., Sun, J.I., Jaime, A., and Lysmer, J., 1988, The Mexico earthquake of September 19,1985-relationship between soil conditions and

earthquake ground motions: Earthquake Spectra, v. 4, p. 687-729.
U.S. Department of Agriculture (USDA), 1981, Transportation engineering handbook, Region 1, supplement 11: Missoula, Montana, U.S. Department of Agriculture, Forest Service, Northern Region.
U.S. Department of Agriculture (USDA), 1996, Soil survey laboratory manual: USDA Natural Resources Conservation Service Soil Survey Investigations Report 42, version 3.0, 693 p.
U.S. Department of Agriculture (USDA), 1994, Slope stability reference guide for national forests in the United States, volume I: Washington, D.C., USDA Forest Service Engineering Staff Report EM-7170-13.
Vokes, H.E., Myers, D.A., and Hoover, L., 1954, Geology of the west-central border area of the Willamette Valley, Oregon: U.S. Geological Survey Oil and Gas Investigations Map OM-150, scale: 1:62500.
Walker, G.W., and Duncan, R.A., 1989, Geologic map of the Salem 1° by 2° quadrangle, western Oregon: U.S. Geological Survey Miscellaneous Investigations Series Map I-1893, scale 1:250000.
Walker, G.W., and MacLeod, N.S., 1991, Geologic map of Oregon: U.S. Geological Survey, scale 1:500000.
Wang, Y. and Leonard, W.J., 1996, Relative earthquake hazard maps of the Salem East and Salem West quadrangles, Marion and Polk Counties, Oregon: Oregon Department of Geology and Mineral Industries Geologic Map Series GMS-105.
Wang, Y. and J.L. Clark, 1999, Earthquake Damage in Oregon: Preliminary Estimates of Future Earthquake Losses, Special Paper 29, Oregon Department of Geology and Mineral Industries, p59.
Wang, Z., Madin, I.P., and Street, R.L., 1998, Shear-wave velocity and soil classifications for communities in Oregon: Proceedings of the 8th International IAEG Congress, Vancouver, British Columbia, Canada, September 21-25, 1998, p. 149-154.
Wang, Z., R. L. Street, E. W. Woolery, and I. P. Madin, 2000, SH-Wave Refraction/Reflection and Site Characterization, Use of Geophysical Methods in Construction (Getechnical Special Publication No. 108), **Proceedings of Sections of GEO-Denver 2000**, ed. By S. Nazarian and J. Diehl, ASCE, Reston, Virginia, p. 126-140.
Wang, Z., and Wang, Y., 2000, Earthquake hazard maps and seismic risk assessment for Klamath County, Oregon: Oregon Department of Geology and Mineral Industries Interpretive Map Series IMS-20, 28 p.
Wang, Z., C.S. Hasenberg, G.B. Graham, and F.N. Rad, 2001, Seismic Hazard and Risk Assessments in Tillamook County, Oregon, Oregon Department of Geology and Mineral Industries (in press).
Weaver, C.S., and Shedlock, K.M., 1989, Potential subduction, probable intraplate, and known crustal earthquake source areas in the Cascadia subduction zone, *in* Hays, W.W., ed., 3rd Annual Workshop on "Earthquake Hazards in the Puget Sound, Portland Area," Proceedings: U.S. Geological Survey Open-File Report 89–465, p. 11–26.
Weiczorek, G.F., Wilson, R.C., and Harp, E.L., 1985, Map showing slope stability during earthquakes in San Mateo County, California: U.S. Geological Survey Miscellaneous Investigations Series Map I-1257-E, scale 1:62,500.

Wiley, T.J., Sherrod, D.R., Keefer, D.K., Qamar, A., Schuster, R.L., Dewey, J.W., Mabey, M.A., Black, G.L., and Wells, R.E., 1993, Klamath Falls Earthquake, September 20, 1993-Including the strongest quake ever measured in Oregon, Oregon Geology, v. 55, p. 127-134.

Yeats, R.S., Graven, E.P., Werner, K.S., Goldfinger, C., and Popowski, T.S, 1991, Tectonics of the Willamette Valley, Oregon, *in* Rogers, A.M., Walsh, T.J., Kockelman, W.J., and Priest, G.R., eds., Assessing earthquake hazards and reducing risk in the Pacific Northwest, volume 1: U.S. Geological Survey Professional Paper 1560, p. 183-222.

Yelin, T.S., Tarr, A.C., Michael, J.A., and Weaver, C.S., 1994, Washington and Oregon Earthquake history hazards: U.S. Geological Survey Open File Report 94-226-B, 11 p.

Youd, T.L. and D.M. Perkins, 1978, Mapping Liquefaction-Induced Ground Failure Potential, Journal of the Geotechnical Engineering Division, ASCE, Vol. 104, No. GT4, p433-446.

Appendix A. SH-wave Velocity Data

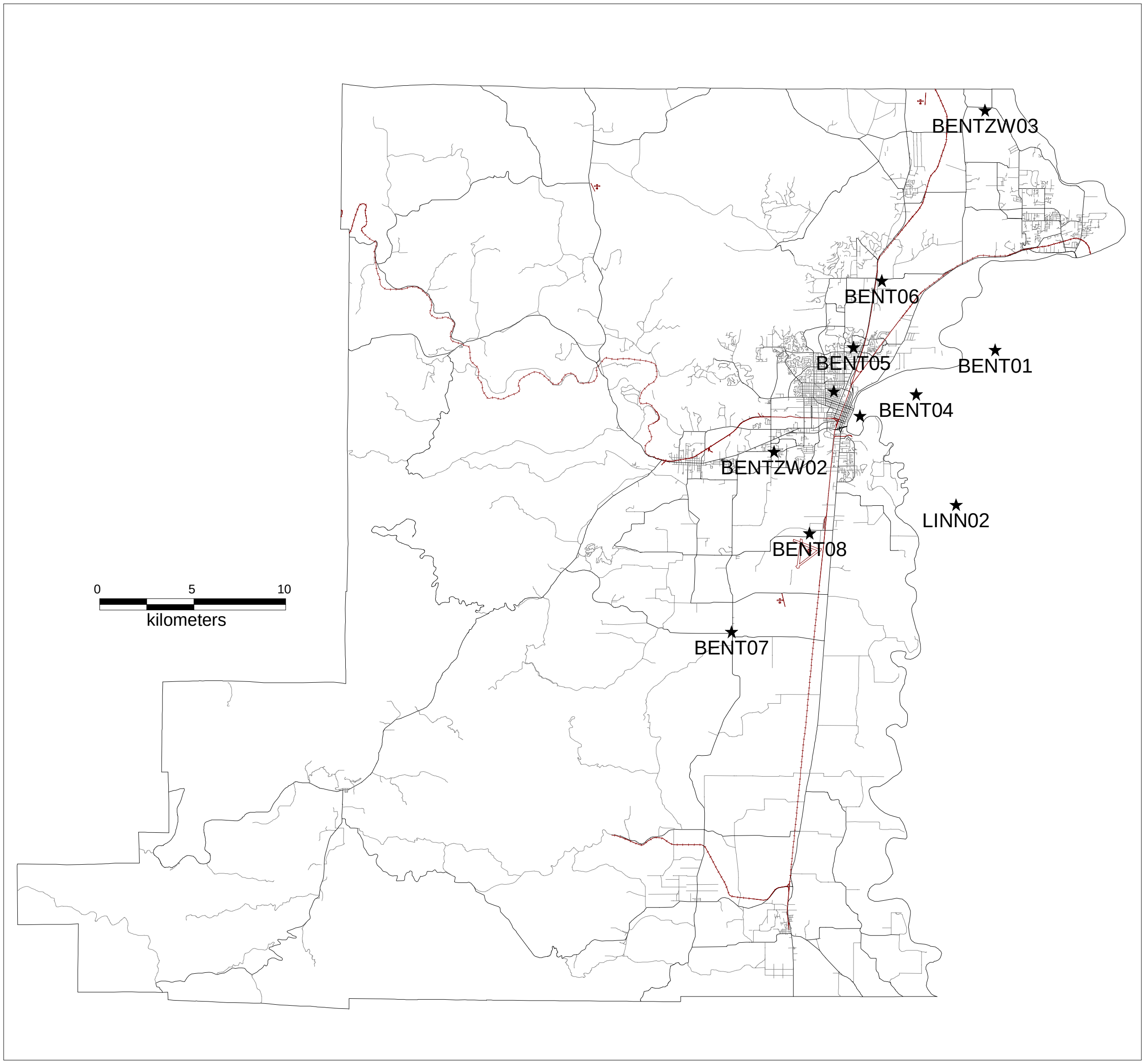

Figure A-1. Locations of geophysical investigation sites.

Table A-1. Shear-wave velocities (m/s).

Site_ID	Vs_Qal	Vs_Qws	Vs_Qlg	Vs_Pal	Vs_BDRX
BENT07	0	164	723	0	0
BENT08	0	239	621	0	0
BENT04	162	0	0	0	490

BENT06	0	162	0	0	575
BENT05	0	180	325	0	0
BENT01	0	178	797	0	0
LINN01	213	0	346	0	0
LINN02	0	166	806	0	0
BENTZW01	0	153	310	403	0
BENTZW02	0	105	615	0	0
BENTZW03	0	129	221	0	0

Appendix B. Building Inventory in Benton County

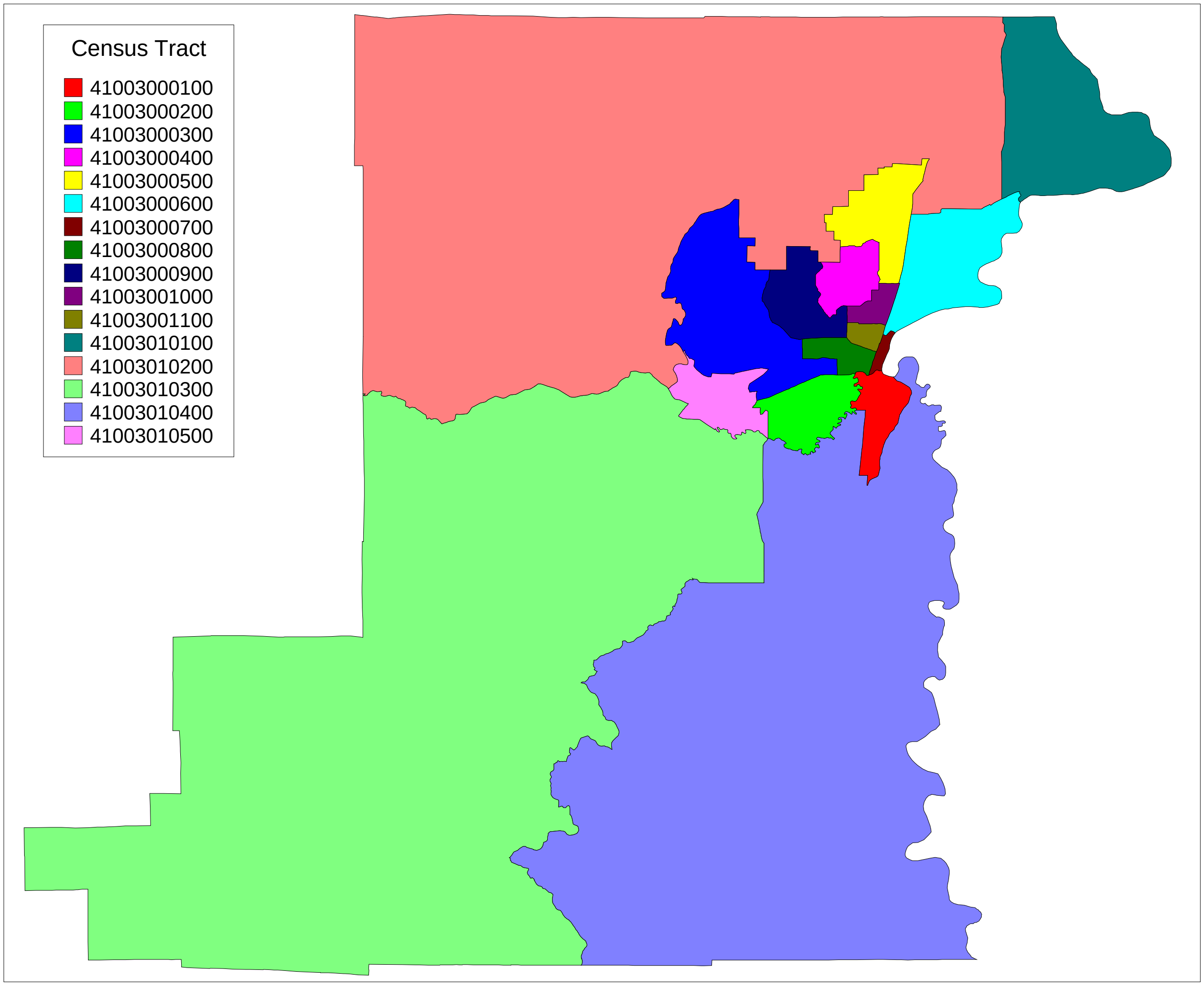

Figure B-1. Census tracts in Benton County.

Table B-1. Building inventory (general occupancy) in Benton County.

TRACT	RES	COM	IND	AGR	REL	GOV	EDU	TOTAL
41003010200	758	4	2	87	5	13	6	875
41003000300	789	4	13	67	5	2	1	881
41003010300	834	14	5	82	2	0	6	943
41003010400	710	9	14	262	3	0	6	1004
41003010500	804	54	15	16	0	0	5	894
41003000700	180	214	10	0	0	11	0	415
41003000100	1516	61	17	3	1	12	2	1612
41003000200	943	29	4	21	1	4	11	1013
41003000400	2804	62	4	0	7	1	2	2880
41003000500	1011	19	4	17	8	0	0	1059
41003000600	1210	87	29	35	2	11	10	1384
41003000800	698	18	2	0	6	1	117	842
41003000900	1905	0	10	1	3	0	8	1927
41003001000	2269	113	2	0	10	1	10	2405
41003001100	1243	80	3	0	20	7	9	1362
41003010100	1422	4	0	62	0	4	5	1497
TOTAL	19096	772	134	653	73	67	198	**20993**

Table B-2. Building inventory (general building type) in Benton County.

TRACT	WOOD	STEEL	CONCRETE	PRECAST	RMASONRY	URMASONRY	MOBILE	TOTAL
41003010200	531	31	9	13	16	10	264	874
41003000300	702	25	6	13	12	11	115	884
41003010300	503	27	7	14	14	10	367	942
41003010400	513	78	13	39	36	16	308	1003
41003010500	765	20	14	17	18	14	47	895
41003000700	219	44	42	38	51	20	2	416
41003000100	1261	22	19	16	20	19	253	1610
41003000200	920	16	10	9	14	13	32	1014
41003000400	2769	18	20	13	21	35	5	2881
41003000500	921	10	6	6	9	12	95	1059
41003000600	720	41	27	31	34	18	514	1385
41003000800	664	41	42	10	62	18	4	841
41003000900	1875	8	8	3	8	21	3	1926
41003001000	2093	29	32	20	33	33	167	2407
41003001100	1226	28	32	16	31	23	4	1360
41003010100	1368	19	4	8	10	17	69	1495
TOTAL	17050	457	291	266	389	290	2249	**20992**

Table B-3. Building value (thousand dollars) per general occupancy in Benton County.

TRACT	RES	COM	IND	AGR	REL	GOV	EDU	TOTAL
41003010200	113196	5978	2583	249	1202	506	4436	128150

41003000300	83069	10316	3242	290	2977	330	1652	101875
41003010300	111976	6443	4218	539	0	484	3408	127068
41003010400	122882	9057	11053	1314	986	513	3619	149424
41003010500	120898	29855	8034	202	1559	454	5659	166661
41003000700	78909	93076	6483	242	2310	183	1773	182977
41003000100	177694	37413	11388	384	1737	682	2453	231751
41003000200	80395	9891	5027	715	1352	315	7059	104755
41003000400	246452	24939	1545	70	4423	894	3562	281885
41003000500	116942	76604	2455	223	8019	469	2607	207319
41003000600	133947	17337	44339	569	1709	528	3578	202007
41003000800	387054	22826	4324	94	4761	1107	2704	422870
41003000900	213152	8219	1155	137	338	748	0	223749
41003001000	287430	65463	2232	199	5474	1019	5610	367428
41003001100	478821	57818	3030	174	13944	1297	6365	561448
41003010100	208876	15171	3755	334	939	843	3756	233674
TOTAL	2961693	490406	114863	5735	51730	10372	58241	**3693041**

Table B-4. Building value (thousand dollars) per building type in Benton County.

TRACT	WOOD	STEEL	CONCRETE	PRECAST	RMASONRY	URMASONRY	MOBILE	TOTAL
41003010200	101175	3368	3072	2273	3092	1981	13190	128150
41003000300	79458	4807	3539	2323	3981	2054	5713	101875
41003010300	96108	3359	2479	2465	2679	1833	18145	127068
41003010400	109572	8058	4709	4654	4662	2518	15253	149424
41003010500	118108	11106	10432	7781	10622	4846	3765	166661
41003000700	85151	20022	23578	16977	24980	10176	2092	182977
41003000100	163281	14640	11729	8470	13167	6256	14208	231751
41003000200	82514	5677	4711	3078	4693	2300	1782	104755
41003000400	241450	9167	9707	3904	9909	5704	2044	281885
41003000500	138615	15670	15556	6361	22726	3413	4978	207319
41003000600	103120	28447	14144	11070	13387	5055	26784	202007
41003000800	226450	36497	74439	6500	50788	22935	5261	422870
41003000900	195867	5053	7420	2019	6332	4411	2647	223749
41003001000	265341	20620	23073	10814	23951	10985	12644	367428
41003001100	339098	43451	75494	11793	58272	25484	7856	561448
41003010100	207156	5359	4702	3492	5351	3879	3736	233674
TOTAL	2552464	235301	288784	103974	258592	113830	140098	**3693041**

Table B-5. Average square footage (thousand square feet) for specific occupancy types.

SPECIFIC OCCUPANCY	DESCRIPTION	AVERAGE SQUARE FEET PER BUILDING	HAZUS DEFAULT VALUES
RES1	Single Family Dwelling	1.56	1.50
RES2	Mobile Home	1.00	1.00
RES3	Apartment/Condo	12.50	16.00
RES4	Temporary Lodging	33.60	50.00
RES5	Institutional Dormitory	43.30	30.00
RES6	Nursing Home	45.00	45.00
COM1	Retail Store	8.40	14.00
COM2	Warehouse	10.60	35.00
COM3	Personal/Repair	5.10	12.00
COM4	Office	7.60	35.00
COM5	Bank	9.50	22.00
COM6	Hospital	143.00	95.00
COM7	Medical Office	4.40	12.00
COM8	Entertainment	5.10	13.00
COM9	Theater	13.20	17.00
COM10	Parking	9.00	9.00
IND1	Heavy Industry	25.00	50.00
IND2	Light Industry	29.20	20.00
IND3	Food/Drug	21.00	21.00
IND4	Metals/Minerals	16.00	16.00
IND5	High Technology	250.00	17.00
IND6	Construction	1.50	19.00
AGR1	Agriculture	8.20	14.00
REL1	Religion/Church	20.90	15.00
GOV1	General Government	12.00	25.00
GOV2	Emergency Response	12.00	10.00
EDU1	K-12 Schools	35.00	20.00
EDU2	College/University	47.50	25.00

Appendix C. Damages and Losses

C-1. Damages and Losses From the M 6.5 Corvallis Fault Scenario

Table C-1-1. Expected building damage by general occupancy.

TRACT	OCCU	NONE	SLIGHT	MODERATE	EXTENSIV	COMPLETE
41003010200	RES	442	179	113	22	3
	COM	3	0	0	0	0
	IND	1	1	0	0	0
	AGR	53	17	14	3	0
	REL	3	1	1	0	0
	GOV	9	3	1	0	0
	EDU	3	1	1	0	0
	TOTAL	**514**	**202**	**130**	**25**	**3**
41003000300	RES	508	186	82	15	1
	COM	3	0	0	0	0
	IND	8	3	2	0	0
	AGR	40	14	11	3	0
	REL	3	1	1	0	0
	GOV	2	0	0	0	0
	EDU	1	0	0	0	0
	TOTAL	**565**	**204**	**96**	**18**	**1**
41003010300	RES	468	210	137	21	0
	COM	9	1	1	0	0
	IND	4	1	1	0	0
	AGR	50	17	12	3	0
	REL	1	0	0	0	0
	GOV	0	0	0	0	0
	EDU	4	1	1	0	0
	TOTAL	**536**	**230**	**152**	**24**	**0**
41003010400	RES	273	197	176	59	7
	COM	3	1	2	1	0
	IND	4	3	4	3	0
	AGR	101	61	65	30	5
	REL	1	1	1	0	0
	GOV	0	0	0	0	0
	EDU	2	1	1	1	0
	TOTAL	**384**	**264**	**249**	**94**	**12**
41003010500	RES	537	186	70	13	1
	COM	34	8	8	3	0
	IND	8	3	3	1	0
	AGR	9	3	2	1	0
	REL	0	0	0	0	0
	GOV	0	0	0	0	0
	EDU	3	1	1	0	0
	TOTAL	**591**	**201**	**84**	**18**	**1**
41003000700	RES	66	61	40	9	0
	COM	45	41	71	46	15

	IND	2	2	3	2	1
	AGR	0	0	0	0	0
	REL	0	0	0	0	0
	GOV	3	2	4	3	0
	EDU	0	0	0	0	0
	TOTAL	**116**	**106**	**118**	**60**	**16**
41003000100	RES	500	489	379	125	22
	COM	13	11	21	14	3
	IND	3	3	6	4	0
	AGR	1	1	1	1	0
	REL	0	0	0	0	0
	GOV	3	2	4	2	0
	EDU	1	0	1	0	0
	TOTAL	**521**	**506**	**412**	**146**	**25**
41003000200	RES	452	308	161	26	2
	COM	10	5	8	3	0
	IND	1	1	1	1	0
	AGR	9	5	5	2	0
	REL	0	0	0	0	0
	GOV	1	1	1	0	0
	EDU	5	2	3	1	0
	TOTAL	**478**	**322**	**179**	**33**	**2**
41003000400	RES	1923	646	205	34	1
	COM	35	12	11	2	0
	IND	2	1	1	0	0
	AGR	0	0	0	0	0
	REL	4	1	1	0	0
	GOV	1	0	0	0	0
	EDU	1	0	0	0	0
	TOTAL	**1966**	**660**	**218**	**36**	**1**
41003000500	RES	466	321	185	37	4
	COM	7	5	5	1	0
	IND	1	1	1	1	0
	AGR	6	4	4	2	0
	REL	3	2	2	1	0
	GOV	0	0	0	0	0
	EDU	0	0	0	0	0
	TOTAL	**483**	**333**	**197**	**42**	**4**
41003000600	RES	299	324	333	205	51
	COM	17	17	27	21	6
	IND	5	4	9	8	2
	AGR	9	8	9	6	2
	REL	0	0	1	0	0
	GOV	3	2	3	3	1
	EDU	3	2	3	2	0
	TOTAL	**336**	**357**	**385**	**245**	**62**

41003000800	RES	256	242	161	36	3
	COM	4	4	6	3	1
	IND	0	0	1	0	0
	AGR	0	0	0	0	0
	REL	1	1	2	1	0
	GOV	0	0	0	0	0
	EDU	27	19	38	27	8
	TOTAL	**288**	**266**	**208**	**67**	**12**
41003000900	RES	1306	438	139	22	1
	COM	0	0	0	0	0
	IND	7	2	1	0	0
	AGR	1	0	0	0	0
	REL	2	0	0	0	0
	GOV	0	0	0	0	0
	EDU	5	1	1	0	0
	TOTAL	**1321**	**441**	**141**	**22**	**1**
41003001000	RES	1053	727	407	81	9
	COM	35	24	34	16	1
	IND	1	0	1	0	0
	AGR	0	0	0	0	0
	REL	3	2	3	1	0
	GOV	0	0	0	0	0
	EDU	3	2	3	1	0
	TOTAL	**1095**	**755**	**448**	**99**	**10**
41003001100	RES	463	440	279	61	5
	COM	16	15	28	14	4
	IND	0	0	1	0	0
	AGR	0	0	0	0	0
	REL	5	4	6	4	1
	GOV	2	1	3	1	0
	EDU	2	2	2	1	0
	TOTAL	**488**	**462**	**319**	**81**	**10**
41003010100	RES	701	447	231	41	3
	COM	2	0	0	0	0
	IND	0	0	0	0	0
	AGR	25	14	15	8	0
	REL	0	0	0	0	0
	GOV	2	0	1	0	0
	EDU	2	1	1	1	0
	TOTAL	**732**	**462**	**248**	**50**	**3**

Table C-1-2: Expected Damage to Essential Facilities

Classification	**Total**	**# Facilities**

		With At Least Moderate Damage	With Complete Damage	With Functionality > 50% at day 1
Hospitals	2	2	0	2
Schools	31	31	0	4
EOCs	1	1	0	0
Police Stations	6	6	0	6
Fire Stations	6	6	0	2

Table C-1-3: Expected Damage to the Transportation System

System	Component	Number of Locations				
		Locations/ Segments	With At Least Mod. Damage	With Complete Damage	With Functionality > 50 %	
					After Day 1	After Day 7
Highway	**Roads**	30			30	30
	Bridges	24	1	0	24	24
	Tunnels	0	0	0	0	0
Railways	**Tracks**	41			41	41
Bus	**Facilities**	1	0	0	1	1
Airport	**Facilities**	7	2	0	7	7
	Runways	7	0	0	7	7

Table C-1-4: Expected Damage to the electric system

	Total # of Households	Number of Households without Service				
		At Day 1	At Day 3	At Day 7	At Day 30	At Day 90
Electric Power	26,256	17,182	9,904	3,630	170	26

C-2. Damages and Losses From the 500-Year Probabilistic Ground Shaking Scenario

Table C-2-1. Expected building damage by general occupancy.

TRACT	OCCU	NONE	SLIGHT	MODERATE	EXTENSIV	COMPLETE
41003010200	RES	326	215	156	46	19
	COM	1	0	0	0	0
	IND	1	1	0	0	0
	AGR	35	20	20	8	5

	REL	2	1	1	0	0
	GOV	5	3	3	1	1
	EDU	2	1	1	0	0
	TOTAL	**372**	**241**	**181**	**55**	**25**
41003000300	RES	445	219	101	24	9
	COM	1	0	1	0	0
	IND	5	2	3	2	0
	AGR	30	14	14	5	4
	REL	2	1	1	0	0
	GOV	1	0	0	0	0
	EDU	0	0	0	0	0
	TOTAL	**484**	**236**	**120**	**31**	**13**
41003010300	RES	299	244	193	68	35
	COM	5	1	4	1	0
	IND	1	1	1	0	0
	AGR	30	19	20	8	5
	REL	1	0	0	0	0
	GOV	0	0	0	0	0
	EDU	3	1	1	1	0
	TOTAL	**339**	**266**	**219**	**78**	**40**
41003010400	RES	231	189	166	78	52
	COM	1	1	2	1	0
	IND	3	2	4	3	1
	AGR	79	59	62	36	25
	REL	1	1	1	0	0
	GOV	0	0	0	0	0
	EDU	2	1	1	1	0
	TOTAL	**317**	**253**	**236**	**119**	**78**
41003010500	RES	478	225	85	18	5
	COM	19	10	14	5	2
	IND	5	3	4	1	1
	AGR	7	4	3	2	0
	REL	0	0	0	0	0
	GOV	0	0	0	0	0
	EDU	2	1	1	0	0
	TOTAL	**511**	**243**	**107**	**26**	**8**
41003000700	RES	73	60	38	5	3
	COM	28	37	61	50	39
	IND	1	2	3	2	2
	AGR	0	0	0	0	0
	REL	0	0	0	0	0
	GOV	2	2	3	3	2
	EDU	0	0	0	0	0
	TOTAL	**104**	**101**	**105**	**60**	**46**
41003000100	RES	538	471	334	103	71
	COM	7	10	19	13	11

	IND	3	3	5	3	3
	AGR	1	1	1	0	0
	REL	0	0	0	0	0
	GOV	2	2	4	2	2
	EDU	0	0	1	0	0
	TOTAL	**551**	**487**	**364**	**121**	**87**
41003000200	RES	437	314	162	18	17
	COM	5	5	9	5	2
	IND	1	1	1	1	0
	AGR	6	5	5	3	2
	REL	0	0	0	0	0
	GOV	0	1	1	1	0
	EDU	3	2	3	2	2
	TOTAL	**452**	**328**	**181**	**30**	**23**
41003000400	RES	1806	757	237	8	4
	COM	23	13	15	5	1
	IND	2	1	1	1	0
	AGR	0	0	0	0	0
	REL	3	1	1	1	0
	GOV	0	0	0	0	0
	EDU	1	0	0	0	0
	TOTAL	**1835**	**772**	**254**	**15**	**5**
41003000500	RES	472	317	163	31	24
	COM	6	4	5	5	1
	IND	1	1	1	1	0
	AGR	6	4	4	3	1
	REL	3	2	2	1	1
	GOV	0	0	0	0	0
	EDU	0	0	0	0	0
	TOTAL	**488**	**328**	**175**	**41**	**27**
41003000600	RES	301	307	295	181	127
	COM	11	15	26	21	14
	IND	4	4	9	8	5
	AGR	8	8	9	6	5
	REL	0	0	0	0	0
	GOV	2	2	3	3	1
	EDU	2	1	3	2	2
	TOTAL	**328**	**337**	**345**	**221**	**154**
41003000800	RES	279	236	144	24	15
	COM	2	2	5	5	2
	IND	0	0	1	1	0
	AGR	0	0	0	0	0
	REL	1	1	2	1	1
	GOV	0	0	0	0	0
	EDU	18	18	35	27	21
	TOTAL	**300**	**257**	**187**	**58**	**39**

41003000900	RES	1173	530	178	23	1
	COM	0	0	0	0	0
	IND	4	2	4	0	0
	AGR	1	0	0	0	0
	REL	2	1	1	0	0
	GOV	0	0	0	0	0
	EDU	4	1	1	0	0
	TOTAL	**1184**	**534**	**184**	**23**	**1**
41003001000	RES	1117	701	340	67	50
	COM	21	23	35	20	12
	IND	0	0	1	0	0
	AGR	0	0	0	0	0
	REL	3	2	3	1	1
	GOV	0	0	0	0	0
	EDU	3	2	3	1	1
	TOTAL	**1144**	**728**	**382**	**89**	**64**
41003001100	RES	508	428	252	35	23
	COM	11	14	22	19	14
	IND	0	0	1	0	0
	AGR	0	0	0	0	0
	REL	4	4	5	4	3
	GOV	1	1	1	1	1
	EDU	2	2	2	1	1
	TOTAL	**526**	**449**	**283**	**60**	**42**
41003010100	RES	759	433	190	30	9
	COM	2	0	0	0	0
	IND	0	0	0	0	0
	AGR	22	14	15	8	5
	REL	0	0	0	0	0
	GOV	2	0	1	0	0
	EDU	2	1	1	1	0
	TOTAL	**787**	**448**	**207**	**39**	**14**

Table C-2-2: Expected Damage to Essential Facilities

Classification	Total	# Facilities		
		With at Least Moderate Damage	With Complete Damage	With Functionality > 50% at day 1
Hospitals	2	2	0	0
Schools	31	31	0	0
EOCs	1	1	0	0
Police Stations	6	6	0	6
Fire Stations	6	6	0	0

Table C-2-3: Expected Damage to the Transportation System

System	Component	Number of Locations				
		Locations/ Segments	With at Least Mod. Damage	With Complete Damage	With Functionality > 50 %	
					After Day 1	After Day 7
Highway	Roads	30			30	30
	Bridges	24	1	0	24	24
	Tunnels	0	0	0	0	0
Railways	Tracks	41			41	41
Bus	Facilities	1	0	0	1	1
Airport	Facilities	7	2	0	7	7
	Runways	7	0	0	7	7

Table C-2-4: Expected Damage to the electric system

	Total # of Households	Number of Households without Service				
		At Day 1	At Day 3	At Day 7	At Day 30	At Day 90
Electric Power	26,256	14,567	7,030	2,033	70	26